



THE UNIVERSITY
of
WISCONSIN
MADISON

FINAL REPORT: REDUCING WHOLE-BODY
VIBRATIONS IN NEONATAL TRANSPORT

May 3rd, 2023

BME 301

Clients: Dr. Ryan McAdams and Dr. Joshua Gollub

Advisor: Dr. Melissa Skala

Team Members:

Team Leader: Joshua Varghese

Communicator: Meghan Horan

BWIG: Sydney Polzin

BPAG: Joey Byrne

BSAC: Nicole Parmenter

Acknowledgements:

BME 200/300 Neonatal Transport Team, Fall 2022

Abstract

Transport puts extreme stress on neonates, who are often in critical condition, lowering their chance of survival [1]. Vibrational forces experienced by neonates during transport have been linked to increased odds of severe brain injury. In particular, intraventricular hemorrhaging (IVH) can lead to neurodevelopmental impairment or death [2], [3]. However, there is no standardized device to mitigate vibrational forces during neonatal transport. To resolve this issue, a spring and damper combination was pursued to help mitigate the harsh vibrations. A total of four separate spring and damper components are placed in parallel between the inner and outer trays of the transport isolette. Accelerometer and gyroscope data was collected from within the isolette both with and without the dampers in order to quantify the effect of the dampers on the magnitude and direction of vibrations. The analysis was focused on the acceleration data for vibrations in the z-direction using MATLAB, and the results were displayed as power spectral density plots. The device demonstrated some reduction in the amplitude of vibrations experienced by the neonate across all frequency ranges, with 42.4% of the frequencies being significant at an alpha of 0.05. Further optimization of the spring constant and damping coefficients and as well as an improved testing protocol will be pursued in the future to further enhance performance.

Table of Contents

Abstract	1
I. Introduction	3
Motivation	3
Existing Devices and Current Methods	3
Problem Statement	6
II. Background	7
Relevant Physiology and Biology	7
Relevant Design Information	8
Client Information	9
Design Specifications	9
III. Preliminary Designs	10
Metal and Gel Composite Continuation	10
Spring Viscous Damper Design	14
Spring and Damper Design	17
IV. Preliminary Design Evaluation	20
Design Matrix	20
Metal/Gel Composite Damper Design	23
Spring Viscous Damper	24
Spring and Damper	25
Final Design	27
V. Fabrication/Development Process	29
Materials	29
Methods	32
Testing	32
Testing Protocol	32
Testing Results	32
VI. Discussion	37
Implications of Results	37
Ethical Considerations	38
Sources of Error	39
VII. Conclusions	40
Future Work	42
VIII. References	44
IX. Appendix	46
A. Product Design Specifications	46
B. Testing Results from Fall 2022 Prototype	54
C. Fabrication Methods	55
D. Spring & Damper Calculations	56
E. Sorbothane Damping Coefficients	58
F. Expenses and Purchases	59
G. MATLAB Code	60

I. Introduction

Motivation

The quality of transport for critically-ill neonates to a Neonatal Intensive Care Unit (NICU) directly influences chances of survival or morbidity [4]. The critically-ill neonate is often the result of a preterm birth (< 37 full weeks of gestation) or underlying birth defects [5]. One in ten neonates need access to a NICU in the first week of life [6]. 1.3% of neonates are born *ex-utero* and must be transported to a NICU via ambulance or helicopter [7]. The current methods of transport expose a neonate to whole-body vibrations (WBV), translational and rotational motion, and excessive sound [8]. The effects of *ex-utero* transfer are well-documented in studies which conclude that transportation of a neonate significantly increases the odds of severe brain injury (odds ratio of 2.32) and significantly lowers the odds of survival without brain injury (odds ratio of 0.60) [2], [3]. One brain injury of concern is intraventricular hemorrhaging (IVH), which is closely associated with neonatal transport and can lead to subsequent neurodevelopmental impairment or death [9]. Therefore, reducing vibrations, mechanical forces, and excessive sound has the potential to significantly improve the outcomes of neonatal transport. There is no standardized vibration-reducing device used in neonatal transport, reflecting the need for a device that minimizes the environmental stressors transferred through the transport vehicle.

Existing Devices and Current Methods

The current methods of minimizing vibrations and mechanical forces by the UW Hospital's neonatal transport teams involve the use of a Geo-Matrix mattress, a five-point harness, various pillows, and suspension systems. The gel mattress in the incubator is placed directly under the neonate during transport. The five-point harness secures the neonate in place using straps across the shoulders, hips, and thighs [10]. The transport team uses additional pillows and blankets to manipulate the position of the neonate or support the head. The transport vehicle's suspension system as well as the built-in suspension system on the gurney act to reduce forces exerted by the ground.

These methods are insufficient in reducing vibrations and mechanical forces felt by the neonate, as whole-body vibration levels often exceed the recommended 0.315 m/s^2 in adults [11]. No standards have been developed for the recommended maximum vibration levels for neonates, but it can be reasonably assumed that it is significantly less than the level for fully-developed adults. The current method does very little to mitigate vibrations and features many rigid parts directly in contact with one another.

While no vibration-reducing device has been established as a standard for neonatal transport, several products have been created for this purpose. The first is the Quasi-Zero-Stiffness (QZS) Isolator (a1, Figure 1) which identifies and targets low-frequency components as the primary disturbing vibration [12]. This product modifies the incubator control box (a3, Figure 1), located directly below the incubator (a2, Figure 1) by adding four QZS Isolators in each corner of the housing. Each QZS Isolator has a pair of repelling ring permanent magnets (c4 & c5, Figure 1) that are connected in parallel to a coil spring (c9, Figure 1). The inner ring magnet (c4, Figure 1) is fixed to a central rod (c1, Figure 1), while the outer ring magnet (c5, Figure 1) is fixed on the sleeve (c7, Figure 1) that surrounds the rod. The concentric system of ring magnets mitigates the effects of rotational and translational motion and keeps the isolators aligned vertically, allowing the coil spring (c9, Figure 1) to take on most of the weight. Finally, a viscous damper (c10, Figure 1) is added inside the coil spring (c9, Figure 1) to help reduce vibrations and forces in the vertical direction. Although the concept of QZS Isolators is well supported, the design involves substantial alterations to the current transport setup, has a complicated design, and lacks experimental testing to verify its ability to reduce whole body vibrations.

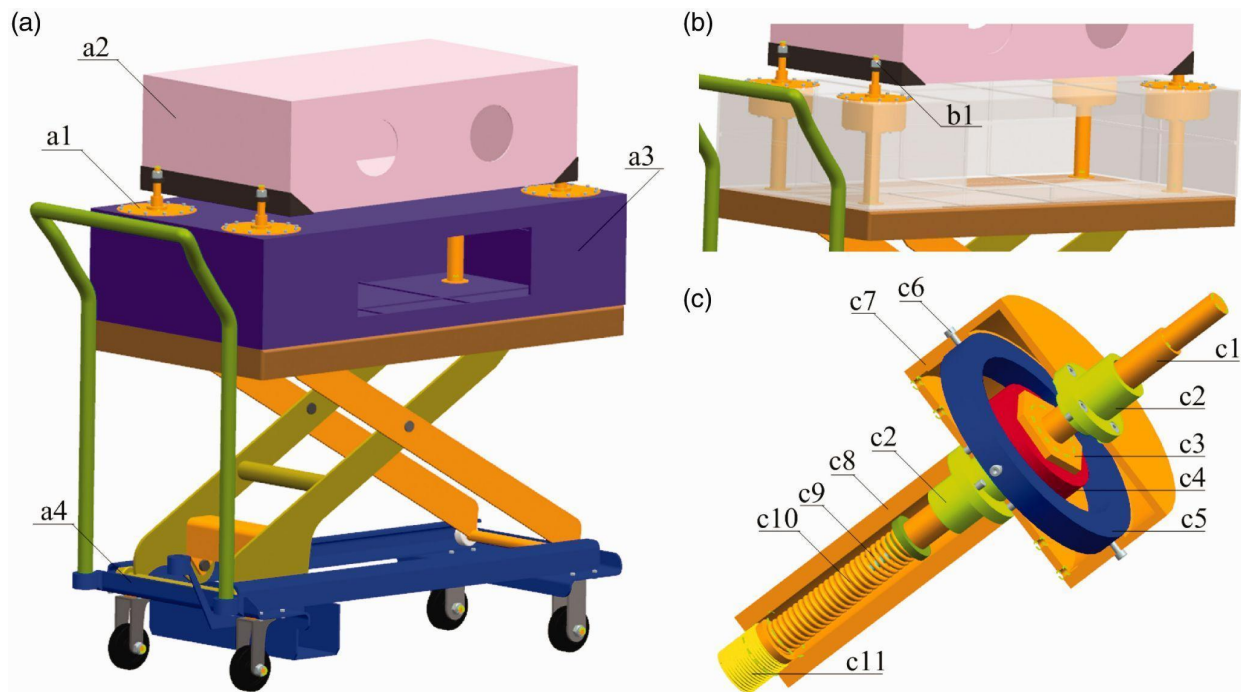


Figure 1: (a) an overview of the QZS vibration isolation system; (b) the installation view of the QZS isolators into the incubator control box; (c) the inside view of the QZS isolator [12].

A second design, referred to as an isolation device for shock reduction occupies the space between the isolette and the stretcher platform, and can be seen in Figure 2 [13]. The design features pairs of metal plates that serve as attachment points for gas or air springs. One plate is mounted to the top of the gurney while the other plate is mounted to the bottom of the isolette. Air or gas springs are fixed between the plates in order to provide dampening effects for the isolette. The pressure within the air springs can be adjusted to attenuate high or low frequencies of vibration. The design specifies that two air springs are placed in each corner and one is placed in the center. A patent application has been submitted for the use of parallel plates and air springs to reduce the transmission of kinetic energy between an isolette and support table (Application Number 11/540743). Similarly to the QZS Isolators, this design involves large modifications to the current transport setup. Additionally, it neglects the presence of the monitoring systems and

associated housing which are located directly below the isolette.

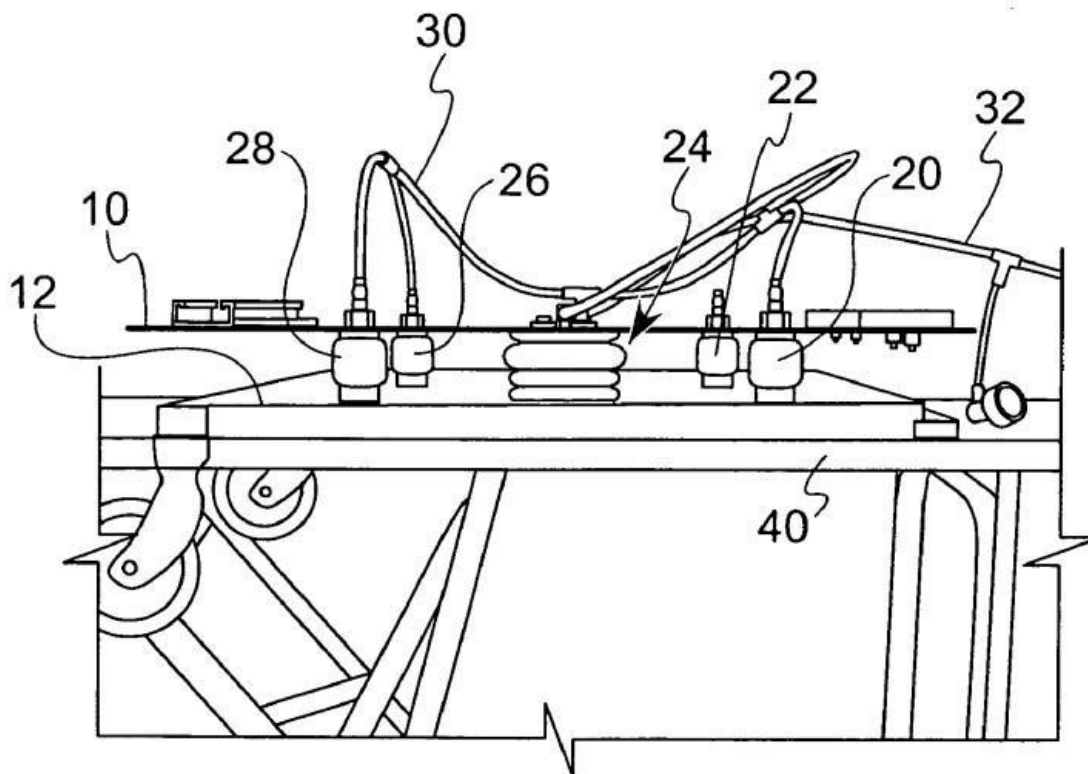


Figure 2: A side view of the isolation device for shock reduction in an operable position on the stretcher platform [13].

Problem Statement

Whole-body vibrations, translational forces, rotational moments, and excessive sound from a medical transport vehicle can cause brain injuries to critically-ill neonates that lead to neurodevelopmental impairment or death. Mitigating these physiological stressors has the potential to drastically improve transport outcomes including increased survival rates and decreased brain injury. The current transport setup neglects the effects of the stressors aforementioned by including a collection of rigid parts and only a single mattress to dampen vibrations. Thus, the client has tasked the team with developing a vibration-reducing device with mitigating mechanical forces and sound as secondary foci. The device must reduce each physiological stressor, so the neonate does not sustain injury, must fit within the dimensions of a standard ambulance and helicopter without interfering with the movement of the transport team,

and must be compatible with current incubator setup or include all the associated functions and equipment (**Appendix A**).

II. Background

Relevant Physiology and Biology

The neonate brain is highly susceptible to injury due to its underdeveloped nature and lack of structural support systems. A neonate's brain is very soft (often compared to unset gelatin) and as a result very vulnerable [14]. Within the brain, neuronal-glia precursor cells make up a vascularized region called the germinal matrix [15]. This region is particularly vulnerable for infants due to weaknesses in the blood-brain barrier in the first 48 hours of life. Moreover, premature infants struggle with cerebral autoregulation, which is the ability of cerebral vessels to keep constant cerebral blood flow (CBF) regardless of changes in arterial blood pressure. The smooth muscle cells and pericytes responsible for minimizing variations of CBF are not fully developed. A fluctuating CBF is associated with pressure passivity in regards to cerebral circulation. Additionally, the neonate's central nervous system is at a very immature stage and is constantly undergoing organizational changes [16]. These changes, combined with physiological instability, limit a neonate's ability to coordinate autonomic and self-regulatory responses towards environmental stressors.

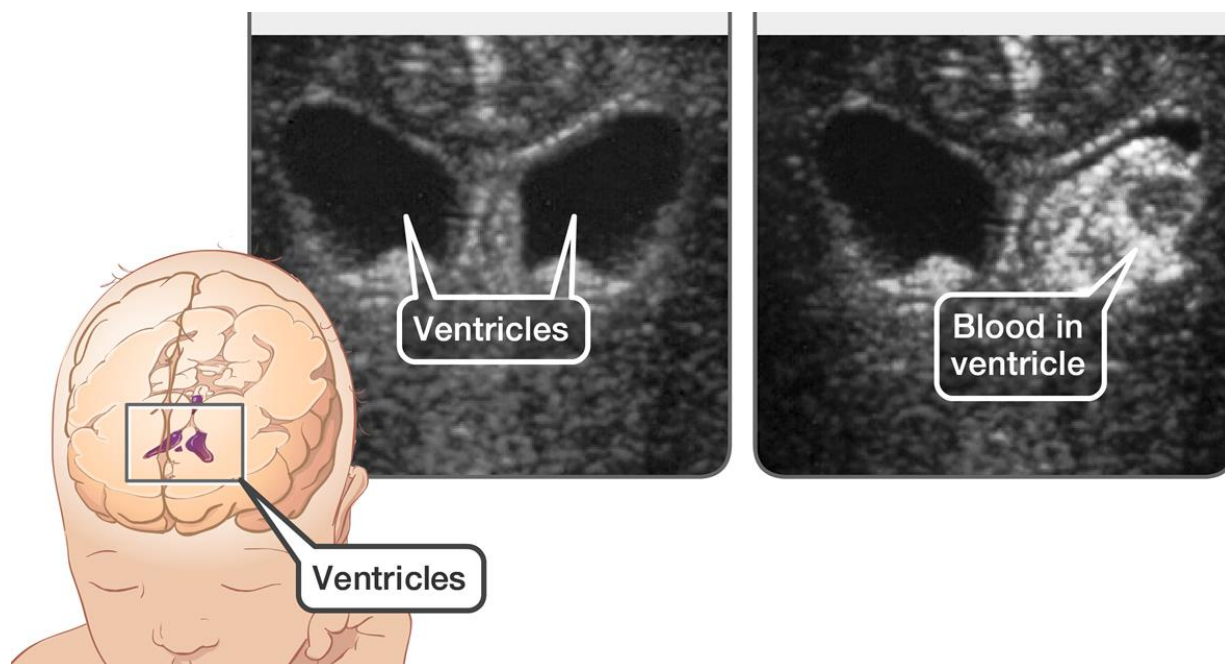


Figure 3: Healthy and IVH CT scans of the neonate ventricles with an anatomical reference on the left [17].

The fragility of a neonate brain described above increases susceptibility to intraventricular hemorrhage (IVH). The capillaries of the highly vascular germinal matrix are especially vulnerable to rupture when the neonate experiences whole-body vibrations [15]. Whole body vibrations can trigger IVH through a cumulative process beginning with cerebral vasoconstriction, increased free radicals, decreased nitric oxide, decreased cerebral blood flow, and repeated reperfusion injury [8]. These characteristics describe the progression of germinal matrix hemorrhage [15], as shown in Figure 3. Furthermore, there is a proven link between fluctuating cerebral blood flow velocity, commonly found in premature neonates, and higher chances of IVH. The nature of ground or air transport in conjunction with the neonate's unstable condition reveals the susceptibility of neonates to brain injury.

Relevant Design Information

The prospective design must function in conjunction with the preexisting setup. Understanding the organization of the transport setup is crucial to understanding design ideas and constraints. Descriptions of the setup are based on observations made from the transport incubator at UW Health, which is International Biomedical's Voyager model [18]. Regardless of

the model, all transport incubators follow the same general structure. The setup includes an incubator (also known as an isolette) which encloses the neonate during transport. A removeable, inner tray supports a mattress and fixes on to a permanent, outer tray on the bottom of the incubator. Below the incubator is metal housing for the incubator's control systems in order to regulate the environment of the incubator (e.g. temperature). This housing, with the incubator latched on top of it, is latched to a transport platform (also known as the deck). Also attached to the deck are a variety of support systems (e.g. oxygen tanks). The deck is then secured onto the gurney for transport.

Client Information

Dr. Ryan McAdams is the Neonatology Division Chief for UW Health and a professor for the UW School of Medicine and Public Health. Dr. Joshua Gollub is a fellow at the University of Wisconsin School of Medicine and Public Health specializing in neonatal medicine.

Design Specifications

The client has tasked the team with developing a device to reduce whole-body vibrations which can cause stress to a neonate during transport in an ambulance. The client requires that the device satisfy several identified problems, which guided the requirements for the project as elaborated in the Product Design Specifications (**Appendix A**). The device must minimize vibrational forces below 0.315 m/s^2 for the entire duration of the transport [11]. The device must mitigate the effects of translational and rotational motion so that the neonate does not sustain injury. The device must attach to the current incubators or include all the associated functions and equipment. Finally, the device must fit within the dimensions of a standard ambulance while allowing efficient movement of the transport team. Due to the constant nature of vibrations and motion during transport, the design should provide continuous functionality without disrupting the support systems and monitoring equipment. In terms of ergonomics, the device should be relatively easy to install and remove and require no additional manipulation once installed. The goal was to create a pilot model (i.e. functional prototype) that can be tested in mock ambulance transports and be implemented as part of the standard transport equipment.

III. Preliminary Designs

The team brainstormed several solutions to address the problem of reducing whole body vibrations to provide neonates with an improved chance of survival. The team decided on three designs to be formally illustrated and evaluated, each with distinct properties and methods to reduce vibrations.

Metal and Gel Composite Continuation

The first design considered was a damping system that consisted of metal and gel concentric layers. The goal of the damper design was to reduce the magnitude of varying frequencies of vibrational forces that are exerted on the neonate during transport. The forces the neonate would have experienced are then dissipated and applied to the tray inside the isolette. This design consists of four inserts that are placed in between the inner and outer trays of the isolette, as shown in Figure 4. There are two side dampers, which are placed in between the two trays and can be seen in Figure 5. These act to reduce the side to side motions and vibrations experienced. There are also two L-shaped dampers, which are placed through a small opening of the inner tray and rest between the two trays. These help to reduce the forwards and backwards motions and vibrations experienced. All four inserts are placed on the neonate accessible end of the trays in case of a medical emergency, such as the need to intubate the neonate during transport. The reason the dampers are placed on the accessible end of the trays is for easy removal and so the dampers reduce vibrations closest to the head of the neonate.

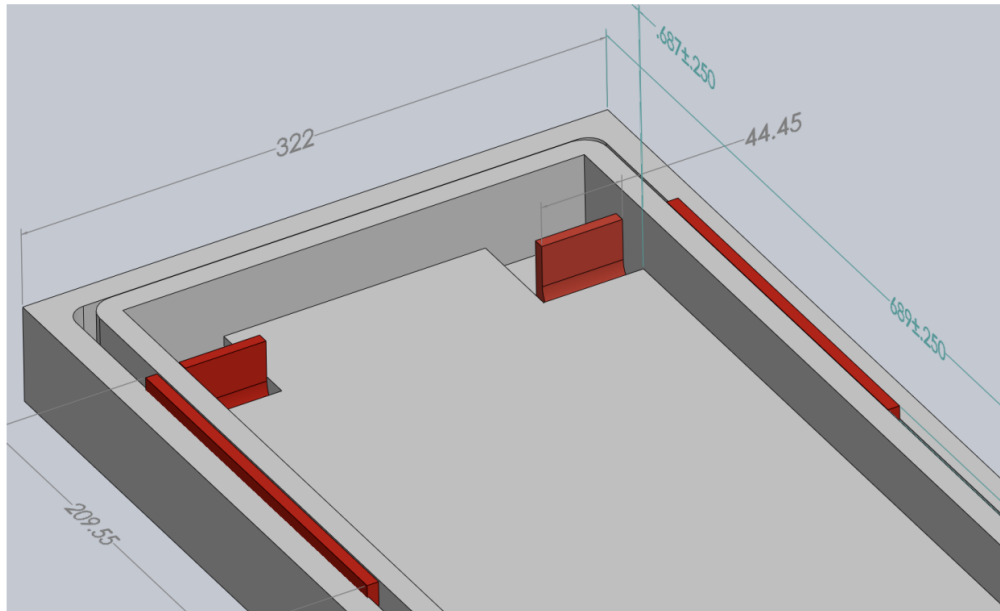


Figure 4: A SolidWorks model of the Metal and Gel Composite Damper placed in the isolette inner and outer trays. Dampers are outlined in red. All dimensions are in mm.

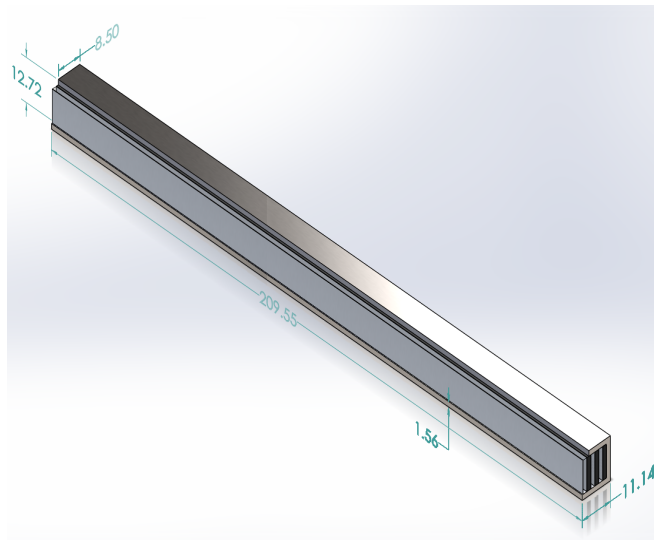


Figure 5: An individual SolidWorks model of the side Metal and Gel Composite Dampers. All dimensions are in mm.

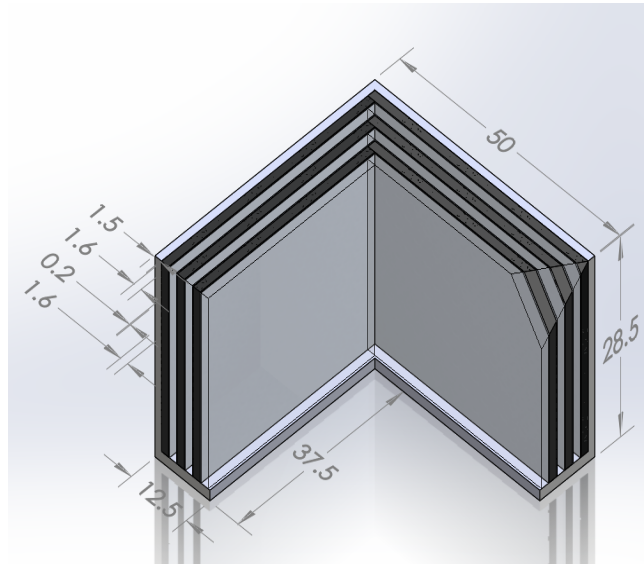


Figure 6: An individual SolidWorks model of the corner Metal and Gel Composite Dampers. All dimensions are in mm.

Each damper is composed of a total of four materials in the same repeating order. There are three repeating layers of foam, aluminum, gel, and aluminum, all enclosed by a single layer of stainless steel. The rationale behind these choices was based on the ability of the layered materials to mimic the unique and natural vibration-reduction properties of a woodpecker's head structure, as shown in Figure 7 [19]. Woodpeckers have a unique layering of bones in their head that enables them to exert significant vibrational forces on their beaks without those same forces having an impact on the brain.

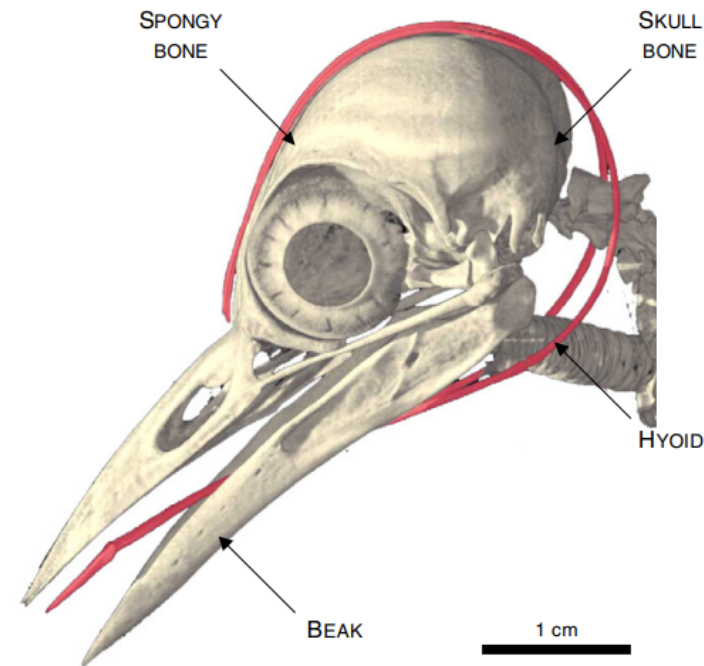


Figure 7: Four key vibration-reducing features of the woodpecker head structure are shown: the beak, the hyoid, skull bone, and spongy bone [20].

There are four main components to the head structure of a woodpecker, including the hyoid, the skull bone, the spongy bone, and the beak, as shown in Figure 7. Each of these components have various functions. The hyoid provides structure to the tongue and the skull bone with cerebrospinal fluid. Each of the four components of the overall head structure of a woodpecker were correlated to man-made materials in the work of Biju et. al (Table 1), who utilized the natural vibration reduction properties of woodpecker anatomy to construct and test shock-absorbing structures.

Table 1: The materials that were correlated to anatomical features of the woodpecker are shown below [19].

Woodpecker	Layered shock absorbing structure
Beak	Metal (steel) enclosure I
Hyoid	Viscoelastic layer (foam)
Spongy bone	Metallic Beads
Skull bone with CSF	Metal (aluminium) enclosure II

This experimental study formed the basis of the Metal and Gel Composite Damper design. The foam layer represents the hyoid, aluminum represents the skull bone with cerebrospinal fluid, gel represents the spongy bone, and the stainless steel outer layer represents the beak. The materials chosen for this design had similar material properties to those shown in Table 1 and can be visualized in Figure 8. The first layer is foam, which is thicker than the other layers included in the damper. This layer of foam is surrounded by a single, thin layer of aluminum, which is then covered with a layer of silicone gel. The gel is covered with a second thin layer of aluminum. Once repeated three times, the damper is enclosed in a single stainless steel layer, forming a medical-grade exterior that is easy to sterilize.

Dampening curves from Biju et. al showed promising results for vibration reduction of this composite material, which can be seen in Figure 10 [19]. Application of this damper for vibrations in an incubator has the potential to be immensely successful.

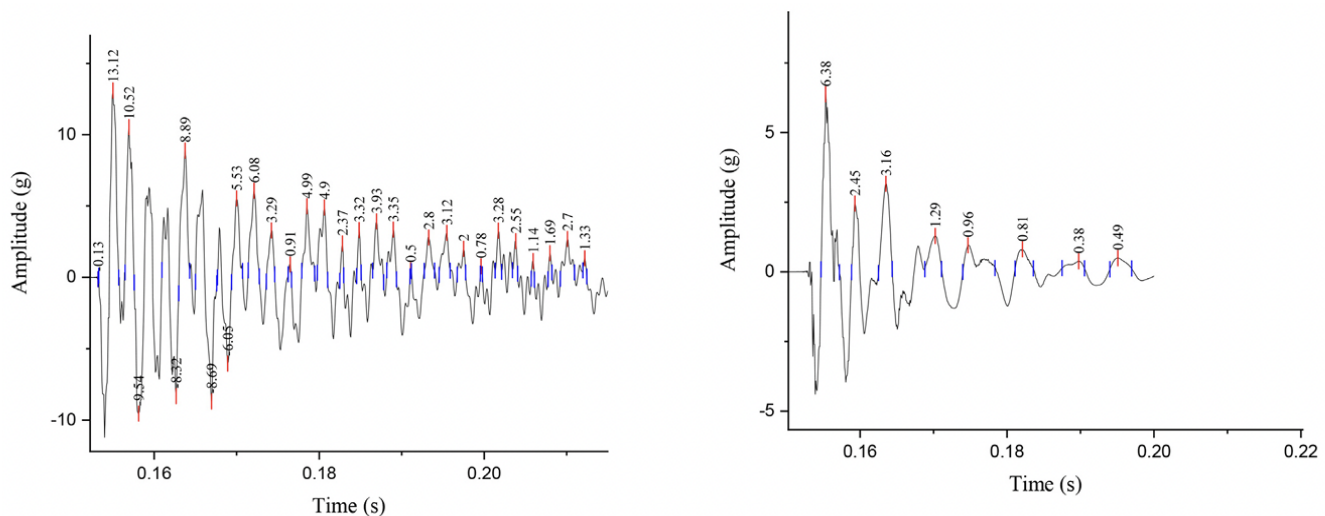


Figure 8: Damping curves for solid stainless steel (left) and the composite damper (right) [19].

Testing was conducted for this mechanism. Results can be seen in **Appendix B**.

Spring Viscous Damper Design

The second design considered was inspired by damper-cable systems used to protect buildings from seismic activity. In these systems, pre-stressed steel cables are connected in series with spring viscous dampers (Figure 9). The cables aid in providing a restorative force after the structure experiences vibrations while the dampers provide energy dissipation capacity [21]. In

buildings, the bearing-end of the damper is connected to the bottom corner of one face of the structure. The connected cable runs horizontally to the opposite corner on the same face of the building. A second damper-cable component is attached in the same fashion to the two remaining corners, creating an “X” shape on the wall of the structure. The damper-cable components in this geometric configuration, as shown in Figure 10, have been found to reduce deformations caused by vibrations.

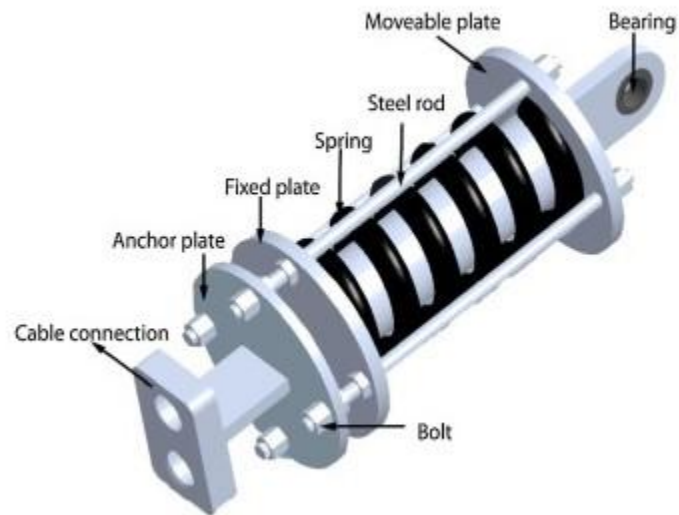


Figure 9: CAD model of the Spring Viscous Damper used in the damper-cable system [21].

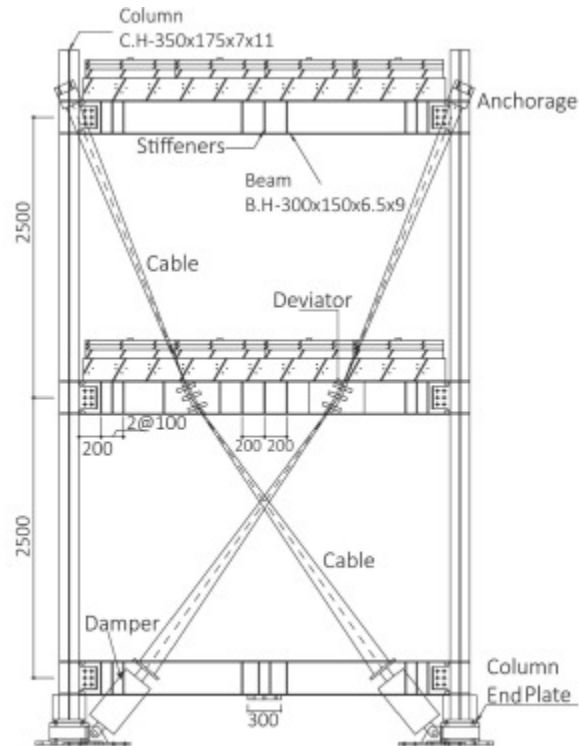


Figure 10: Diagram for implementation of the damper-cable components on a steel structure [21].

In earthquake-resistant buildings, the use of spring-viscous damper systems has been shown to reduce the lateral displacement of the building by up to 70%, and the acceleration of the building by up to 50% during a seismic event [22]. Additionally, spring-viscous damper systems can be designed to have a specific response to different types of earthquakes, making them an effective solution for seismic protection in a variety of locations. By utilizing a similar concept, spring-viscous damper systems in the design of neonatal transport incubators can help absorb and dissipate the vibrations, providing a smoother ride and reducing the risk of injury to the neonate.

The configuration of the damper-cable system aforementioned can be implemented similarly in the incubator transport setup (Figure 11). On one end of the viscous damper, the bearing is connected directly to the deck at each corner of the control box (i.e., there are four total damper-cable parts). The attached cable runs diagonally across the lateral face of the control box and attaches to a preexisting hole at the opposite corner. Two damper-cable components are utilized on each lateral face in order to create an “X” shape.

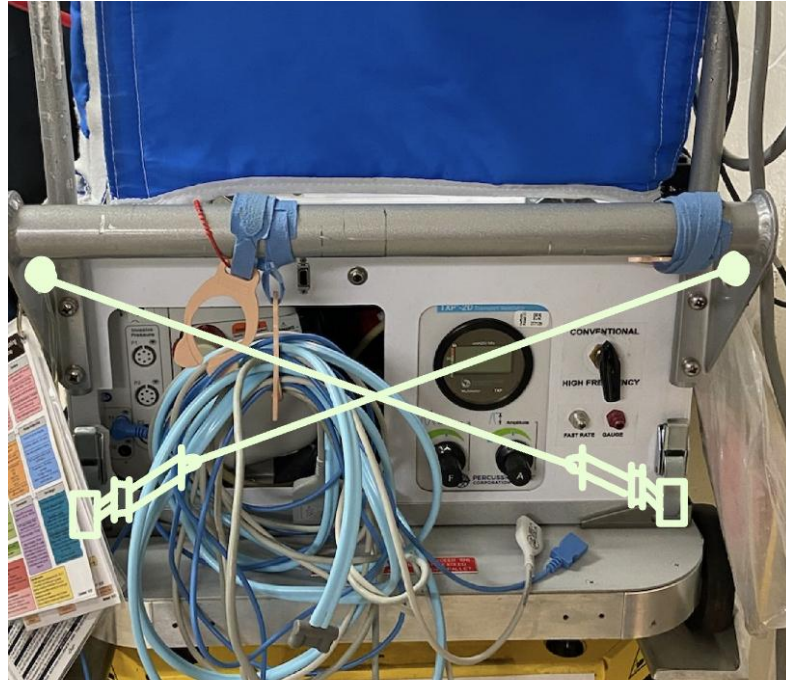


Figure 11: Geometric layout of the damper-cable system on one face of the incubator control box.

Compared to the rigid-nature of the latching mechanism, the Spring Viscous Damper allows for the control box and incubator to move with incoming vibrations via the viscous damper. This flexibility eases the intensity of vibrations felt within the incubator.

Spring and Damper Design

The Spring and Damper design incorporates both a spring and a damper into one system, as shown in Figure 12. The spring component has no internal damping (ideal springs) but stores the energy from vibrations as elastic potential energy [23]. Additionally, the springs provide a restorative force in order to keep the system in the same position that it started in (i.e. zero net displacement). The damper component dissipates the energy stored by the spring and created by the movement from the vibrations. Air or magnetic dampers are both effective solutions for this aspect of the design. Both the spring and damping constants can be tuned to target the disturbance frequency in order to effectively attenuate vibrations [24].

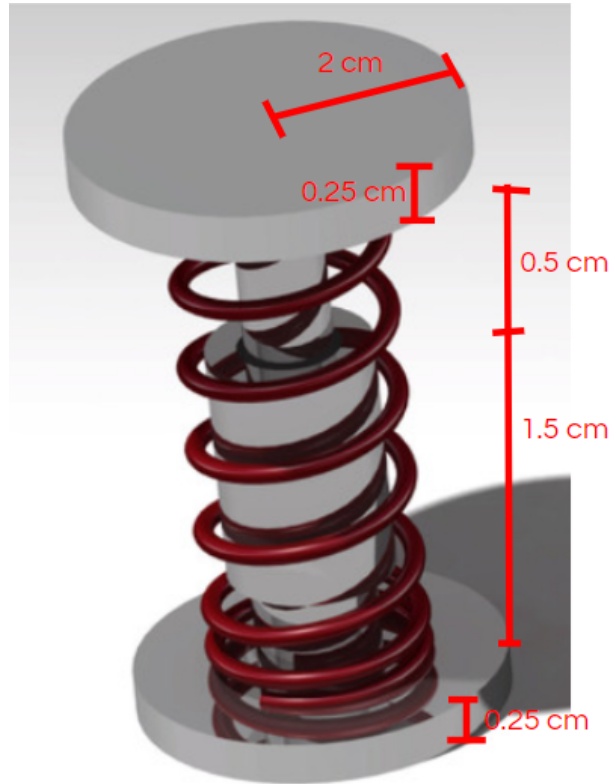


Figure 12: CAD model of the Spring and Damper Design [25]

Similar designs are used in car suspension systems to function as shock absorbers as seen in Figure 13. Irregularities in the road can exert forces to the wheels of a car, causing them to move up and down perpendicular to the road's surface. Therefore, a system is needed to absorb this energy such that it is not transferred to the frame causing the wheels to lose contact with the ground [26].

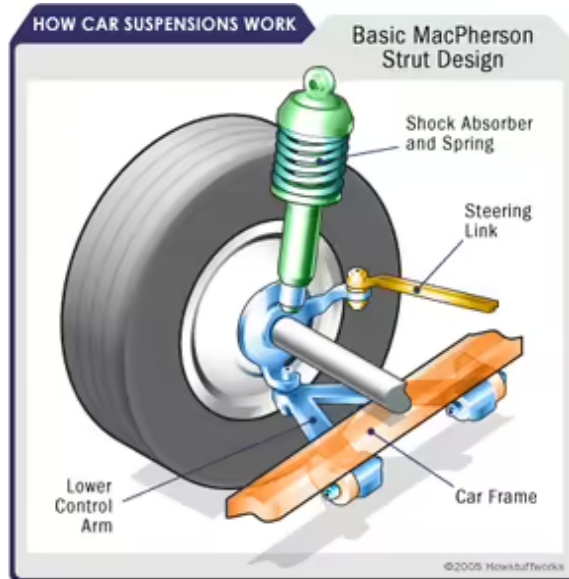


Figure 13: Illustration depicting common strut design, which is a common dampening structure in a vehicle's wheels.

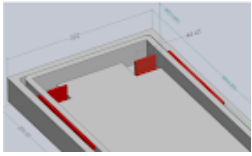
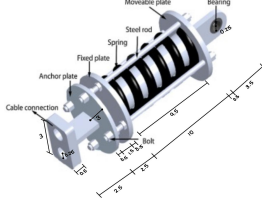
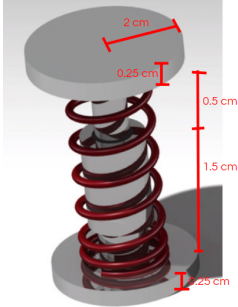
The stiffness of the spring determines how the car responds to the energy, either providing a smoother or bumpier ride. In other words, they absorb energy. Dampers are the component that then dissipate this energy, stopping the spring from bouncing at its natural frequency until all the energy put into it is used.

In the transport setup, these dampers would be placed in between the inner and outer trays on both sides of the tray, as well as underneath the inner tray. The purpose of this placement is to reduce vibrations and absorb shock in the x, y, and z planes. The spring damper system would need to be small enough to fit in between these trays, and the spring coefficients would be based off of the vibrations experienced in each of the three directions, meaning that the coefficients would likely be different for each location they are placed in. If it is not possible to find or fabricate spring damper systems small enough, redesigning the entire tray would be a potential solution to proceed with this design.

IV. Preliminary Design Evaluation

Design Matrix

Table 2: The design matrix and affiliated criteria used to evaluate the preliminary designs, featuring the Gel Composite Continuation, Spring Viscous Damper, and Spring & Damper designs.

		Metal and Gel Composite Continuation		Spring Viscous Damper Design		Spring & Damper Design	
							
	Weight	Score	Total	Score	Total	Score	Total
Efficacy of Vibration Reduction	25	3	15	4	20	5	25
Accessibility to Neonate	20	4	16	5	20	4	16
Compatibility with Equipment	20	5	20	3	12	4	16
Ease of Fabrication	15	4	12	2	6	3	9
Safety	10	5	10	4	8	5	10
Cost	10	5	10	3	6	4	8
TOTAL	100	83		72		84	

Efficacy of Vibration Reduction:

In order to reduce whole body vibrations in neonatal transport, the product needs to be designed to effectively attenuate or dissipate vibrations. This can involve the use of specialized materials, shock-absorbing mechanisms, or other design features that mitigate vibration. As specified in the Product Design Specifications, an ideal prototype will be capable of reducing vibrations to below 0.315 m/s^2 [11]. Additional factors to consider would involve identifying the specific vibration characteristics that are most harmful to neonates, such as frequency and direction, and then designing the product to address those characteristics. This category was given a weight of 25 and ranked as the most important category since any device that does not meet the performance requirements will not only fail to solve the issue presented but could potentially pose additional risk to the neonate.

Accessibility to Neonate:

Accessibility to the neonate is possible through several hinged doors located around the incubator. It is vital that access to these doors are not restricted or compromised so that the medical team can react and treat the neonate throughout the entire duration of travel. This category is weighted slightly lower, with a score of 20, than the reducing vibrations category because reducing vibrations is the primary focus of this project. A device that successfully reduces vibrations would still have the potential to cause harm to the neonate if medical professionals did not have immediate access to the neonate to provide emergency care while in transport. This explains why accessibility to the neonate is the second most important category, as this device should not increase risk to the neonate in any capacity.

Compatibility with Equipment:

The product needs to be compatible with other equipment used in neonatal care, such as oxygen tanks, ventilators, and monitors. This could involve designing the product to attach securely to existing equipment, or to work seamlessly with other products in a neonatal transport system. The device should be simple and require little to no effort for medical professionals to use. Ideally, the device would not require any significant modification of the existing transport system. This category similarly received a weight of 20 because the device should be able to be used in travel incubators within their daily operating environment of an ambulance or helicopter.

Ease of Fabrication:

Ease of fabrication is defined in this context as the level of difficulty to create a working prototype of the design within the constraints of accessible materials, machinery, and time this semester. This could involve designing the product to be modular, or to use materials that are readily available and easy to work with. Although the focus of this category is on small scale preliminary fabrication, the complexity of manufacturing on a larger scale can also be factored into evaluation of this category as well. This category was given a weight of 15 because feasibility is an important consideration to ensure a testable prototype can be created; however, producing a device that effectively minimizes whole body vibration is the ultimate goal and performance should be prioritized over simplicity.

Safety:

The safety category assesses the potential for the device to cause harm or damage. This could involve designing the product to be impact-resistant, easy to sterilize, or to include fail-safe mechanisms that prevent injury or harm in the event of failure or misuse. Any mechanical, electrical, or chemical elements of the device must not harm the user and should be reliable to use on trips that may last for several hours. This category received a weight 10 since it is expected that all of the evaluated designs should comply with the numerous medical standards and practices that exist to protect patients and healthcare workers.

Cost:

This category is scored based on the expenses of the materials as well as the production cost to make the final product. All levels of prototyping should remain less than a total of \$500. The score for this criteria is less significant to the client compared to the emphasis on safety and projected performance, and is willing to discuss a budget expansion if it is necessary to do so. The main goal is to have a successful prototype that can reduce the level of whole body vibrations experienced by the neonate. Any disposable components of the device should also be considered so that replacing parts of the device regularly does not become a financial burden for the hospital.

The aforementioned criteria have been used to assess the following three designs.

Metal/Gel Composite Damper Design

The Metal/Gel Composite Damper Design is a damper made of a layered material; the inner layer is composed of three repeating layers of a hard foam material, aluminum, silicone gel, and aluminum, all enclosed in a single layer of stainless steel. The damper is fabricated in two L-shaped pieces fitted in the corner under the inner tray and two straight pieces fitted under the lips of the inner tray parallel to the head of the neonate, each inserted between the outer tray and inner tray of the incubator on which the baby is placed during transport.

The material for the damper is modeled after the work of Biju et al., who were inspired by the anatomical characteristics of a woodpecker that mitigates vibrations reaching the brain during rapid pecking motions. They developed a layered material consisting of an inner layer of silicone gel, followed by an aluminum layer, a foam layer, and a final outer stainless steel layer. The damping curves from their tests showed that this layered configuration was successful in mitigating vibrations, so our design attempts to apply their idea to an accessory that can be attached to neonatal transport equipment [19]. The goal of this semester would be to change the materials used and/or the way the device is inserted in between the trays to attempt to increase its efficacy.

This design scored a 3/5 on the efficacy of vibration reduction category. As currently designed and tested, the gel composite damper lacks a spring component which is necessary to dissipate the energy from the vibrations. Since a damping component alone, which just reduces magnitude of vibrations, will not be as effective, this device did not score as high as the others. Additionally, testing results from last semester revealed that this design did not reduce acceleration values within the incubator to be below 0.315 m/s^2 [11].

This design scored a 4/5 on the accessibility to neonate category because the only evident issue is the increase in height to the inner tray system. Since the internal height clearance of the incubator is very low and the hand-holes for accessing the neonate have an even lower height clearance, it is important that the inner tray is not raised a significant amount. Raising the inner tray by 1 cm should not cause any issues with accessing the neonate, but any larger adjustments could jeopardize the ability to treat the neonate during transport.

This design scored a 5/5 on compatibility with equipment since it will not hinder access to the oxygen tanks, monitors, or ventilator systems that may be necessary during transport. Additionally, the materials and components of the device will not damage the inside of the

incubator and should not require any interference once attached to the system. There are no adjustments to the device that the MedFlight Team will need to make to the device, allowing for a seamless transition towards the incorporation of the design.

This design scored a 4/5 on ease of fabrication. The design consists of materials that should be simple to source and is conceptually easy to understand. The most difficult part of the fabrication process will be cutting the material into even thinner sheets since the UW Madison TeamLab does not have the appropriate tools to cleanly work with materials as specified in the design. However, final assembly will be a quick process since attaching the various layers will require a simple spray adhesive.

This design scored a 5/5 on the safety category, because it does not greatly interfere with the incubator and stays out of the reach of the neonate. Since there are no complex mechanical, electrical, or chemical components to this design, it is predicted that the gel composite damper will not pose a threat to the patient or health care provider.

This design scored a 5/5 for cost. This design is small and does not require a large volume of material, given that the proposed thickness is less than one centimeter. Additionally, scrap material from last semester is available to remodel this design which would allow the team to use the rest of the budget on exploring testing devices.

Overall, this design scored a 83 on the design matrix. This design takes into consideration the effectiveness of dampers in absorbing shock as well as the limited amount of space within the incubator to intervene with any kind of accessory. The inspiration behind this design came from the anatomy of a woodpecker, which will be incorporated into the material used in the damper [19]. Although this design was superior in the majority of categories, its inability to effectively reduce the vibrations in the incubator meant that it would not be a suitable option to continue this semester.

Spring Viscous Damper

The Spring Viscous Damper design utilizes cables connected in series with a viscous damper to replace the latches which connect the incubator control box to the deck of the stretcher. On one end of the viscous damper, the bearing is connected directly to the deck at each corner of the control box (i.e., there are four total damper-cable parts). The attached cable runs diagonally across the lateral face of the control box and attaches to a preexisting hole at the

opposite corner. Two damper-cable components are utilized on each lateral face in order to create an “X” shape. Compared to the rigid-nature of the latching mechanism, the Spring Viscous Damper allows for the control box and incubator to move with incoming vibrations via the viscous damper. This flexibility eases the intensity of vibrations felt within the incubator.

The Spring Viscous Damper design scored a 4/5 for its efficacy in reducing vibrations because it works to minimize vibrations from the isolette externally rather than between the two trays. As a result, the device would not as effectively target the specific vibrations experienced by the neonate, but rather by the structure as a whole. However, the viscous damper would still allow for shock absorption and stability.

For a similar reason, the design scored higher in the accessibility to neonate category. The external focus of the design means that nothing regarding the isolette or how the neonate is treated within it would be affected by the device.

In contrast, the viscous spring design scored a 3/5 for compatibility with equipment, losing the category. This is because the device relies on metal cables that are connected to clamps on the isolator to strap the components together. These locations for attachment might not be present on other brands of incubators, making the design extremely specific in nature.

Due to the complexity of the damper component, this design scored a 2/5 for ease of fabrication. The damper consists of a collection of metal parts such as discs, rods, and connectors. Since some of the components are likely not available to buy, fabrication of the damper would require complex machining or possibly welding. For this reason, the Spring Viscous Damper scored the lowest of the three designs in this category.

While all the designs were created with safety as a focus, this design received a 4/5 for this category because of the tension in the cables that connect the device to the incubator. If these were to snap, it could be hazardous both to the healthcare providers in the ambulance and the neonate.

Finally, the design scored a 3/5 for cost. The design is largest by nature, therefore requiring the most materials. If the device were to eventually be commercialized, it would also likely cost more in production and labor.

Spring and Damper

The Spring and Damper design incorporates both a spring and a damper into one system.

These dampers would be placed in between the inner and outer trays on both sides of the tray, as well as underneath the inner tray. The purpose of this placement is to reduce vibrations and absorb shock in the x, y, and z planes. The spring damper system would need to be small enough to fit in between these trays, and the spring coefficients would be based off of the vibrations experienced in each of the three directions, meaning that the coefficients would likely be different for each location they are placed in. If it is not possible to find spring damper systems small enough, redesigning the entire tray would be a potential solution to proceed with this design.

The Spring and Damper design scored a 5/5 for efficacy of reducing vibrations because it includes both a damping component and an oscillating (spring) component. Both components are necessary for maximum reduction of vibrations. Additionally, these spring and damper components can be placed on the bottom and sides of the incubator, reducing vibrations in the x, y, and z directions. It is also possible to interchange both the spring and damper components to accommodate different frequencies should these values vary.

This design scored a 4/5 for accessibility to the neonate. While the spring dampers chosen will be as short as possible while still providing the desired vibration reduction effect, they will ultimately lift the inner tray toward the top of the isolette slightly, resulting in less space for medical professionals to reach the neonate. There will still be sufficient room to care for the patient, but this slightly reduced space led to a lower rating in this category compared to designs that do not reduce space inside the isolette.

This design scored a 4/5 for compatibility with the equipment. Pursuing this design would not require a full remodeling of the incubator, but the inner tray in the isoletter may need to be modified depending on the height of the spring dampers. Additionally, this design would not alter the functionality of any other equipment in the ambulance or helicopter, so it would be able to be used with said equipment. Consequently, this design received a good rating, but not the highest possible score.

This design scored a 3/5 for ease of fabrication. As previously mentioned, this design may require a redesign of the inner tray in the isolette which could include altering its dimensions and redesigning the track that allows it to be pulled out of the outer tray. Also, spring dampers that are purchased would likely need to be modified once calculations are completed to determine the desired resistance of the damping portion. Another reason this category received a

lower score is actually connecting the spring damper into the inner tray. If the inner tray material is too brittle to simply screw the spring damper into, a different approach will be required to integrate the spring dampers into the tray system.

This design scored a 5/5 for safety, as the design does not introduce any additional risks to the patient or the current procedure of transporting neonates. This design should be compliant with current medical standards. There are no electrical or chemical components to this design, decreasing potential safety risks.

The design scored a 4/5 for cost. The prices for spring damper systems vary based on size, material, damping type, and spring coefficients. Spring dampers in general are relatively cheap and would fit within the budget; however, potential modifications will likely need to be made to adjust these components, which could increase the price.

Final Design

After evaluating several proposed designs, the team decided to proceed with the Spring and Damper design as the final solution for reducing vibrations during neonatal transport. This design incorporates both a damping and oscillating component, and can be placed in multiple locations to effectively reduce vibrations in all three directions. It is also safe and compatible with existing medical standards, making it a viable option for neonatal transport. While this design slightly reduces space for medical professionals, the team believes that these trade-offs justify the prospective efficiency in vibration reduction. In comparison to the Metal and Gel Composite Design and the Spring and Viscous Damper design, the Spring and Damper design proved to be the most effective and promising solution.

The final design is made up of four 4" x 4" components that work in tandem to provide vibration mitigation to the system. The 1/8" thick HDPE plastic base holds both the spring and damper in place in each of the four corners between the outer and inner trays of the isolette. A Smalley® carbon steel, flat wire spring is placed in the corner closest to the corner of the tray it resides in. Filling the remaining surface area is the Sorbothane® viscoelastic polymer (1/10"-40-DURO-Black Sheet) acting as the damping material. The total device raises the inner tray by 0.572 cm. The damper serves as a natural adhesive to remain in contact with the HDPE base. The spring is fixed to the base by being threaded through three equidistant holes. The knot holding the spring in place was then superglued to the base to prevent movement, fraying, and slippage.

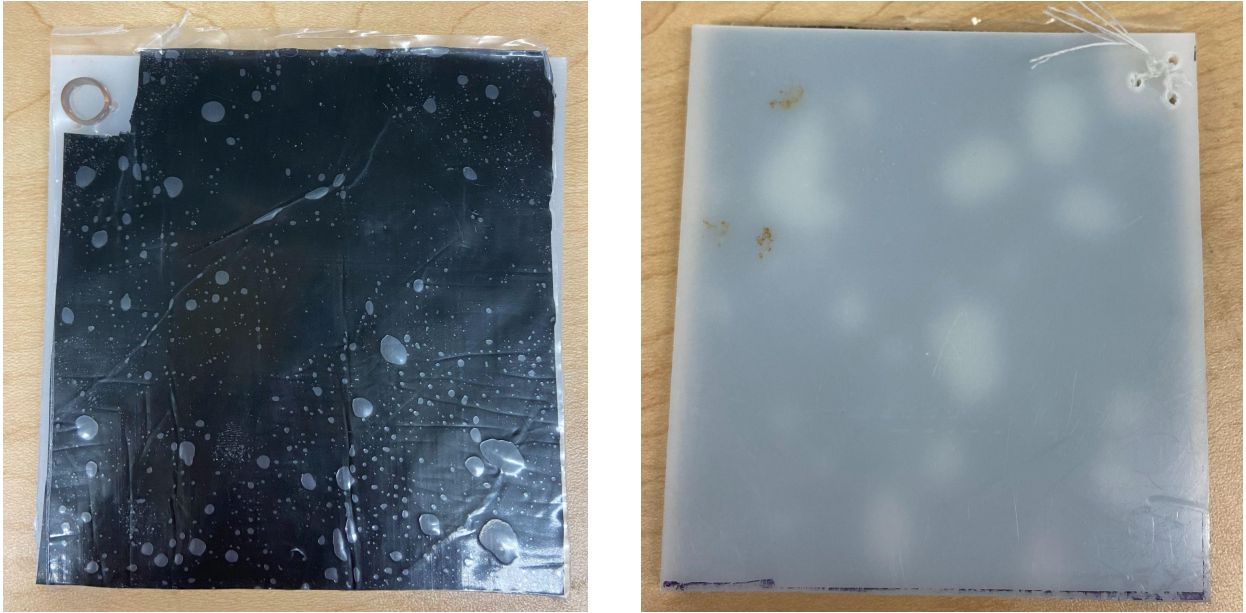


Figure 14: Image of the top (left) and bottom (right) of one of the four components of the final prototype. Note the plastic film on the top surface is kept for storage purposes and is removed upon usage to add friction between the device and tray and ensure its stability.

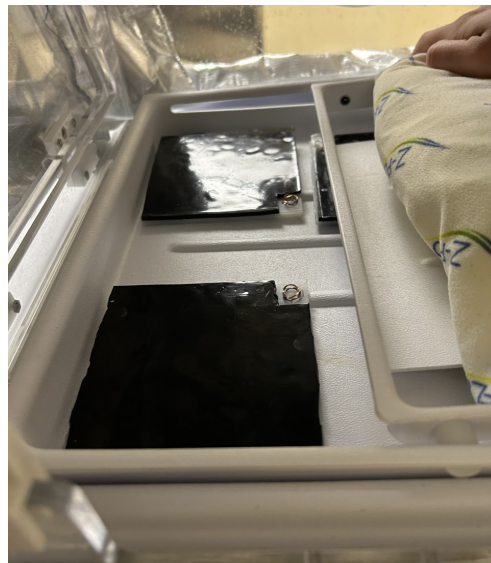


Figure 15: Image of 2/4 of the device components placed on top of the outer tray, with the inner tray pulled forward to reveal them. Each spring is placed on the centermost inside corner. The plastic is removed to allow the adhesive damper to cling to the inner tray.

V. Fabrication/Development Process

Materials

The major materials needed for the design are for the spring and damper components. The springs are made from carbon steel to maximize durability while minimizing cost, given that they are less expensive than stainless steel springs [27]. Additionally, the springs are made from flat wire to allow for smaller compression of the spring, minimizing the vertical raise of the inner tray and thus mitigating any additional complications that could arise while providing care to the neonate during transport.

The springs selected for this design were the Smalley® C037-L1 crest-to-crest springs, shown in Figure 16 below. Each spring has an external diameter of 0.375", a free height of 0.150", and a working height of 0.062".

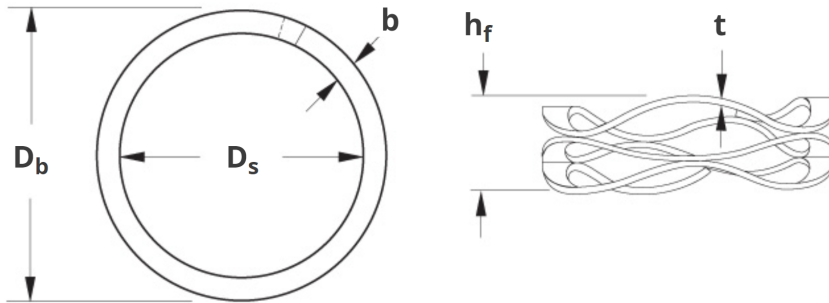


Figure 16: Technical drawing of the C037-L1 spring used in the final prototype. [28]

Additionally, each spring has a spring constant of 7880.70 N/m. Using 4 springs in series, the total device will then have a combined spring constant of 31,522.8 N/m. The spring constant required by the system was found to be 31,692.4 N/m (Equation 1). This was calculated through the following assumptions and calculations:

$$\frac{\omega}{\omega_n} = \frac{2\Pi f}{\sqrt{k/m}} \quad (1)$$

The ratio of $\frac{\omega}{\omega_n}$ was found to be 3.6 using the displacement transmissibility plot from Figure 17 in Dr. Frank Fronczak's textbook describing forced vibration in systems with a single degree of freedom [29]. It operates under two assumptions: a damping ratio of 0.3 and a displacement in the z direction of 0.2. These values were selected under recommendation of Dr. Fronczak as a starting point; however, the optimized values will need to be determined experimentally over time. The damping ratio is a value between 0 and 1 that is defined as the ratio of the actual damping coefficient to the critical damping coefficient. A damping ratio of 0.3 means that the system is underdamped, and is thus characterized by oscillations that decay gradually over time. This is ideal for a spring-mass-damper system because the spring can respond to the input more efficiently to dissipate the energy of the vibrates that occur. The displacement value reflects the distance the mass is displaced relative to its equilibrium position. A value of 0.2 was selected to account for the inevitable movement of the inner tray and neonate in the vertical direction, but to minimize this motion significantly. The mass used is the combined mass of all items that will be sitting on top of the springs, including the mass of the neonate, gel mattress, inner tray, and other equipment. This is approximately 6kg. The frequency, f, refers to the excitation frequency of the system. Using data collected from the previous semester's work on the project, included in **Appendix C**, it was found that the vibration frequency most magnified by the current system is around 17Hz. Solving for the spring constant, k, gives 31,692.4 N/m. Each of the 4 springs chosen has a spring constant of 7880.70 N/m, summing to a total spring constant of 31,522.80 N/m when placed in parallel.

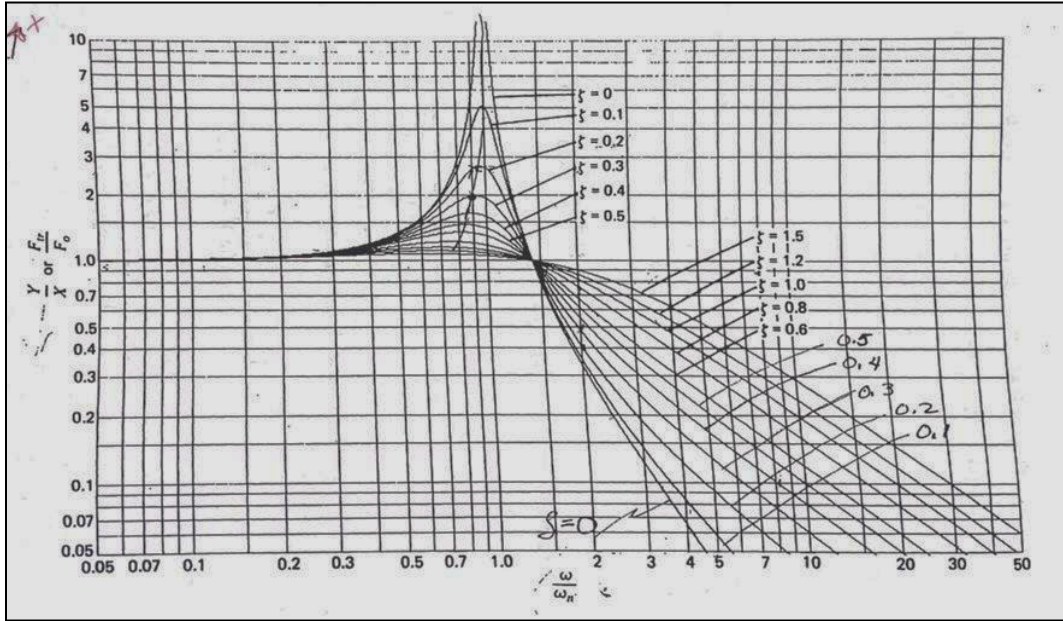


Figure 17: Displacement transmissibility plot used to determine the required spring constant for the springs selected in the final prototype [29].

The damper was selected using Equation 2 to calculate $C_{critical}$, which is the minimum amount of damping required to prevent oscillation.

$$C_{critical} = 2\sqrt{k \times m} \quad (2)$$

Using the previously defined mass of 6 kg and a spring constant of 7880.70 N/m per spring, each damping component should have a $C_{critical}$ of 218 N·s/m, or 1.25 lbf·sec/in. A complete list of all the calculations utilized in this process can be found in **Appendix D**.

Using the specifications provided by Sorbothane® defining the damping coefficients of their various materials, the 40-Durometer sheet stock was selected. As noted in **Appendix E**, it has a damping coefficient of 1.10 to 1.68 at 10% compression within the specified frequency range of 15-30Hz. This provides a range that the desired damping coefficient falls well within to account for any error or confounding variables.

Finally, all materials are able to withstand regular ethanol cleaning and sterilization within degradation over the course of the product's lifespan.

Methods

After obtaining the materials described in the Materials section, four 4" x 4" squares of HPDE were cut out of a larger sheet. The Smalley C0371-L1 springs have three points of contact with the surface they rest on, so three holes were drilled through the HPDE to align with those contact points to ensure that the spring rested flat on the surface. Three pieces of thread were used to loop through the bottom turn of the spring and secure it to the HPDE base through the three holes. The thread was tied in a knot under the base and super glued to ensure that the thread stayed in place and would not unravel.

4" x 4" squares of Sorbothane were cut out to cover the HDPE, with a 1" x 1" region out of one corner of each of the squares to account for the section where the spring was secured. The Sorbothane pieces had adhesive layers on both sides and one was stuck on each HPDE base piece. One of these spring and damper combination pieces was placed on each corner between the inner and outer tray of the isolette. The second layer of adhesive side was stuck to the bottom of the inner tray to hold everything in place and ensure it did not move during transport.

Testing

Testing Protocol

To measure the strength of the vibrational forces within the resting area of the isolette, the team used the WitMotion WT901SDCL Accelerometer that collected data in the x-, y-, and z-directions at a sampling frequency of 200 Hz. This accelerometer is capable of measuring acceleration to the ten-thousandth of a g and stores data on its 32 GB SD card. The accelerometer was placed under the gel mattress inside the inner tray of the isolette, beneath the spot where the neonate's head rests. Data was collected during two separate 50 minute ambulance rides: one with the final design in the isolette and one control run with the isolette alone. Each ride followed the same route, consisting of local roads, highways, and stop-and-go travel. Text files containing raw acceleration data to be analyzed were obtained for each ride.

Testing Results

Text files containing the raw acceleration data from the accelerometer were obtained and

analyzed in MATLAB using the code presented in **Appendix G**. A fast fourier transform was applied to the vertical (z-direction) acceleration components of each of the two sets of data to compute power spectral density plots in the frequency domain to evaluate the randomized vibrations that occur during transport. A PSD plot is a representation of the frequency concentration of a random signal. It shows the power of the signal as a function of frequency, allowing the team to determine the strength of the vibration experienced by the neonate [30]. The shape of the PSD curve can define the mean acceleration of a random signal at any frequency which is important for evaluating the randomized vibrations that occur during transport. The x-axis denotes frequency values while the y-axis measures the relative power at that frequency.

Figure 18 displays the power spectral density plot of the Fall 2022 prototype and control data. This data was collected in the chest of a mannequin with an iPhone that had a sampling frequency of 100 Hz, so this graph goes to 50 Hz on the x-axis, which is the Nyquist frequency. The data shows that the Fall 2022 prototype reduced some of the power but was more effective in shifting the peaks in power amplitude to lower frequencies. Figure 19 shows the power spectral density plot of the Spring 2023 prototype and control data. Since the data this semester was collected with an accelerometer with a sampling frequency of 200 Hz, this graph ranges from 0 to 100 Hz. A comparison of the points with and without the Spring 2023 prototype reveals an overall reduction in amplitude in power across frequencies. This consistently lower power amplitude with this semester's prototype across the whole graph indicates that using a spring and damper together more reliably lessens vibrations felt in the isolette rather than just using a damping component like the Fall 2022 prototype, which lowers the power in some places, but shifts the power peaks to different frequencies, worsening vibrations in others.

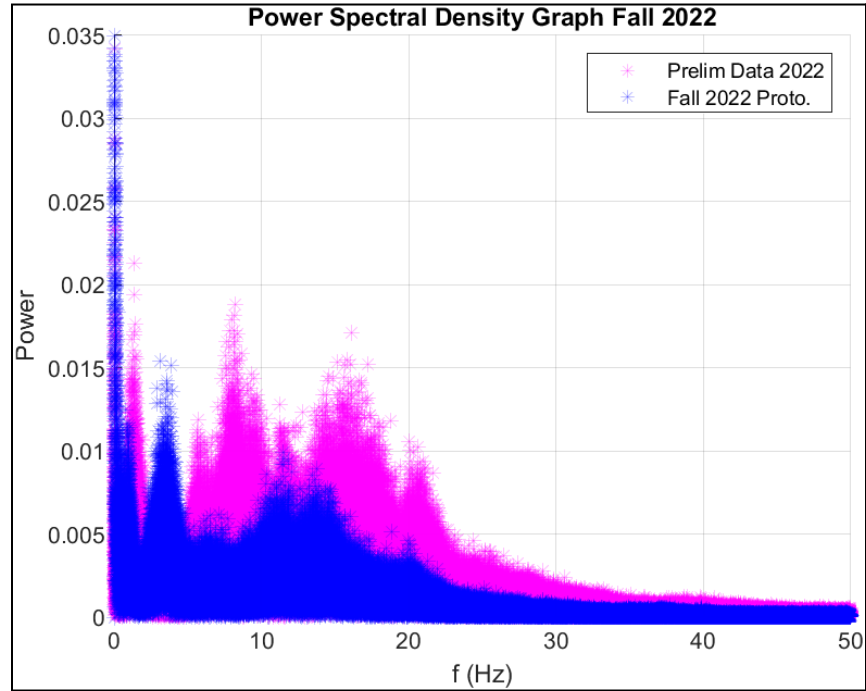


Figure 18: Power spectral density plot of Fall 2022 data with and without Fall 2022 semester prototype.

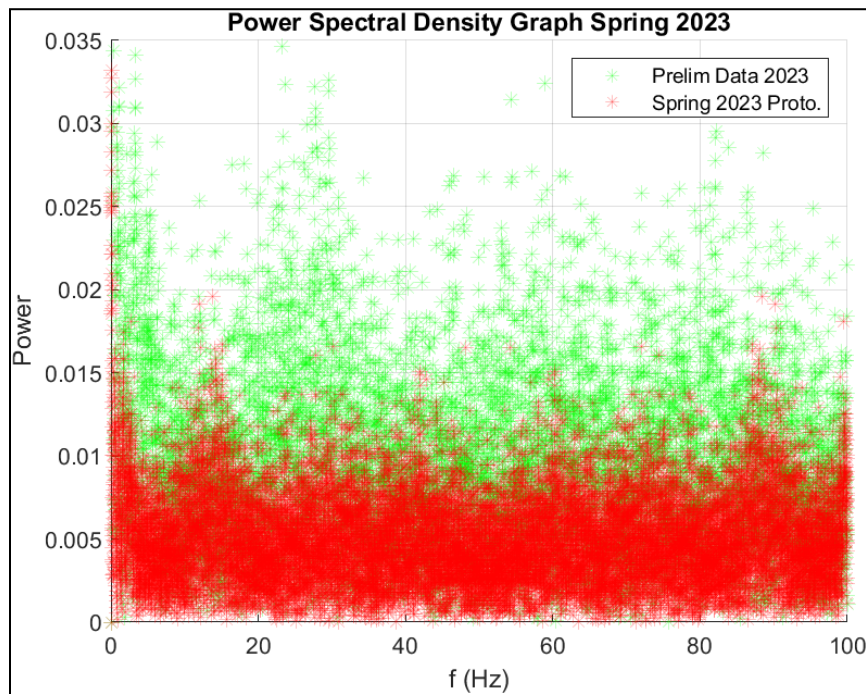


Figure 19: Power spectral density plot of Spring 2023 data with and without the prototype.

Table 3: Count of significant p-values for Fall and Spring Prototypes.

	# of Number of Significant Bins	% Significant
Fall 2022 Prototype	163	65.2%
Spring 2023 Prototype	106	42.4%

To determine the statistical significance of these results, each set of data was separated into 250 bins. A Welch's t-test was performed on corresponding data points from the two PSDs for each bin. Each bin was designated as significant if the p-value was less than 0.05 and the number of significant bins are shown in Table 3. The prototype from last semester had 163 significant bins out of the 250 bins and this semester's prototype had 106 significant bins out of the 250, indicating that there was a more distinct change in vibrations when last semester's prototype was used compared to this semester's. The more significant change when the Fall 2022 prototype is used is due to the shift in large power amplitudes to lower frequencies. When the Spring 2023 prototype is used, the change is less significant, as the power is reduced across all frequencies and not moved to a different frequency.

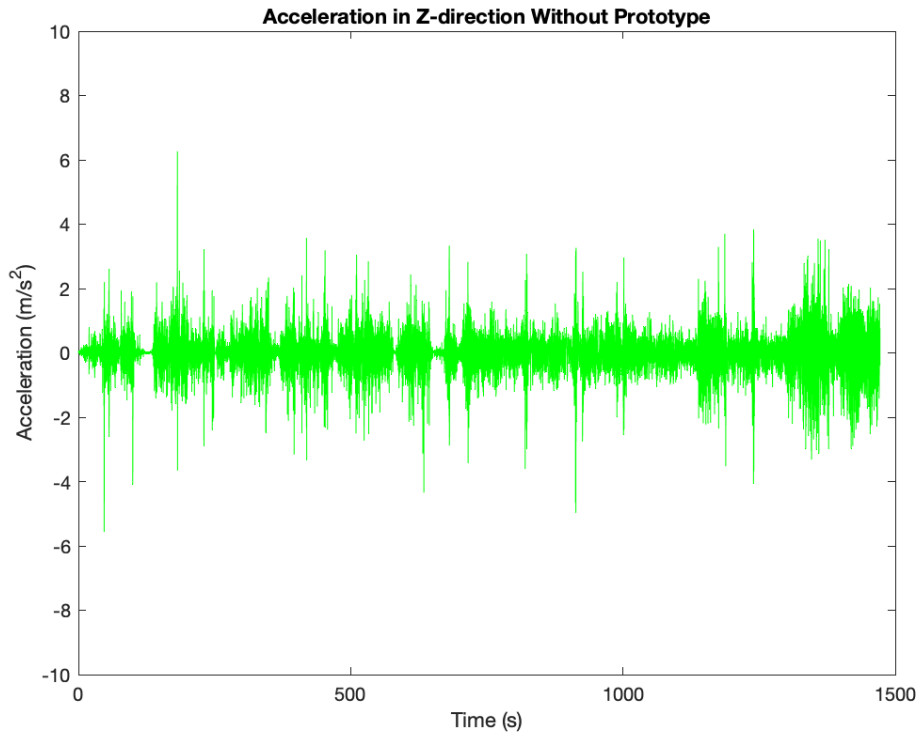


Figure 20: Raw acceleration values for the Z-direction without the prototype.

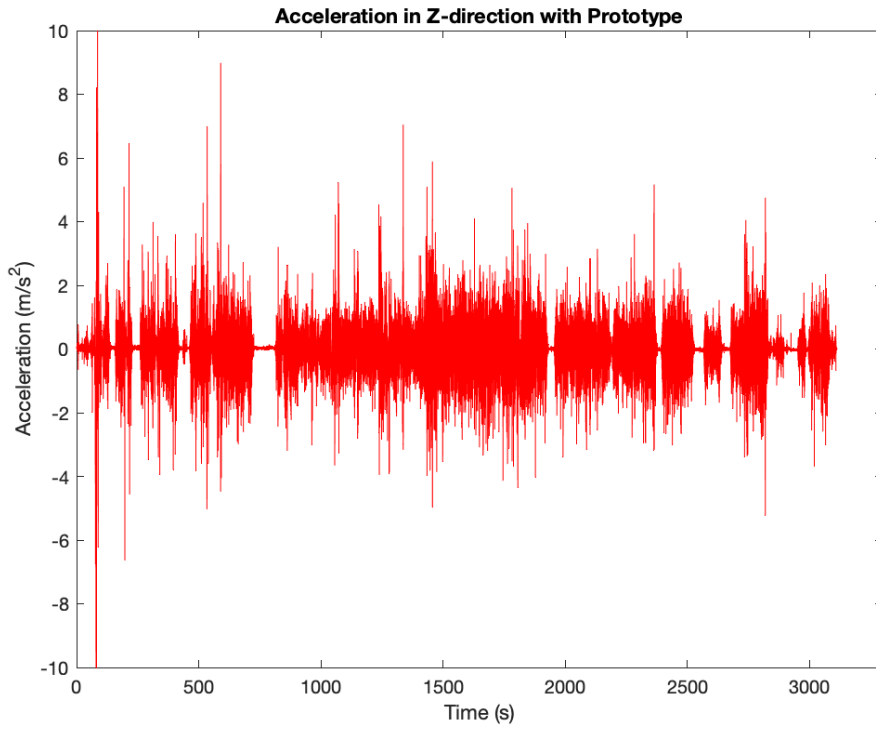


Figure 21: Raw acceleration values for the Z-direction with the Spring 2023 prototype.

The primary test to meet validation by already published literature is to reduce the vibrational accelerations felt by the neonate to be below the recommended 0.315 m/s^2 [11]. The acceleration data depicted in Figures 19 and 20 were used to determine whether this criteria was met. An analysis of the data revealed that, for the entire series of data collected, 23.18% of the acceleration samples exceeded the recommended threshold of 0.315 m/s^2 for the preliminary data. For the data collected using the prototype, this percentage increased slightly to 25.88%.

VI. Discussion

Implications of Results

Following the evaluation of the device's performance during a simulated transport ride utilizing all the necessary transport equipment, the team was able to derive multiple conclusions regarding the gathered data and the effectiveness of the design. The testing results indicated that both the Fall 2022 and Spring 2023 prototypes reduced the power and amplitude of vibrations experienced by the neonate during transport. The Fall 2022 prototype shifted some power amplitude peaks to lower frequencies, while the Spring 2023 prototype consistently reduced power amplitude across all frequencies. Statistical analysis showed that the Fall 2022 prototype had a more significant impact on reducing vibrations than the Spring 2023 prototype (Table 3). However, a closer examination of the significant bins revealed that the Fall 2022 prototype significantly increased, rather than decreased, power in some frequency ranges, inflating the number of significant bins. The Spring 2023 prototype was more effective at reducing vibrations across all frequencies, despite having a lower percentage of significant bins (42.4% compared to 65.2% for the Fall 2022 prototype). As the team seeks to completely eliminate the power of vibrations, a spring and damper combination as presented this semester will continue to be refined due to its ability to dissipate, instead of shift, vibrations in the system.

While the primary test to meet validation by published literature is to reduce the vibrational accelerations felt by the neonate to below the threshold of 0.315 m/s^2 , the team found that the percentage of acceleration samples exceeding the recommended threshold increased slightly with the prototype. Despite the initial expectation that the percentage of time spent above the threshold would decrease with the prototype, the team discovered that factors such as the difference in ride length, stopping at red lights, and traffic patterns had an impact on the

acceleration periods in the data collected. These factors can all vary depending on the driver and may have contributed to the increase in the percentage of samples exceeding the threshold. Therefore, more testing samples from additional rides are required to confirm the significance of the presented findings.

In conclusion, both the Fall 2022 and Spring 2023 prototypes show promise in reducing the vibrational accelerations felt by the neonate during transport. The Spring 2023 prototype consistently reduced the power amplitude across all frequencies, while the Fall 2022 prototype was more effective in shifting the peaks in power amplitude to lower frequencies. However, the increase in the percentage of acceleration samples exceeding the recommended threshold suggests that further evaluation and redesigning is necessary to create a fully functional prototype. Future work will concentrate on conducting more tests to validate the presented findings and optimize the design of the prototypes for use in real-world scenarios.

Ethical Considerations

In the development of a new medical device, ethical considerations must be addressed in regards to research, patient safety, and inclusivity. First, ethics surrounding medical research involves acting on sufficient information and understanding and using that information to promote well-being [31]. The quantity and quality of research must be sufficient in providing an accurate, complete description of the problem and design variables in order to make informed decisions. Understanding of the research is just as critical as the team needs to act as experts in the identified field. A final focus of research ethics is reporting the research honestly and giving credit where it is due. Medical devices operate on the basis of the truth of the research done and will inevitably fail if research is falsified.

Secondly, medical ethics address the importance of patient safety and health through official device approval and testing. It is important to prove device efficacy prior to use to ensure that the device will function as intended. To do so, the device must comply with the standards set for Class II medical devices according to the FDA and receive approval prior to use (**Appendix A**) [32]. Additionally, the use of HDPE outer coating will protect existing equipment from the magnetic field generated by the magnetic damper while also allowing these components of the design to be easily removed and sterilized using an autoclave or ethylene oxide [33]. In regards to testing, it is important that results are reported transparently and all results are included.

Omitting negative test results falsely informs clients and patients about device efficacy and can result in device failure during use.

Finally, inclusivity is an important ethical consideration which allows all patients to have the access and ability to use the device. Thus, religious, cultural, and economic considerations were taken into account during development of the final prototype. The chosen materials are permitted among all known cultures and religions which may forbid the use or interaction with certain substances. Finally, the cost of the device is kept low to allow accessibility to clients and patients regardless of economic status. Ethical considerations were taken into account throughout the design process and guided decisions to create a well-informed prototype.

Sources of Error

As in any iterative design process, the team encountered challenges that could have caused errors in the development, testing, and analysis of the device. Primarily, there are judgements made in the calculations required to determine the spring constant and damping coefficient. These judgments will need to continue to be optimized from experimental data in order to better refine these measurements. Additionally, they rely on several assumptions including the following: the system operates in a single degree of freedom, the mass of the inner tray, mattress, and neonate is a point mass, and the springs are massless and without hysteresis. Any of these factors could create inconsistencies in the calculations for these components. Finally, the springs selected were small in both height and diameter to mitigate the extent to which the inner tray was raised in the upper tray and therefore maximize the available space for healthcare providers to treat a neonate in transport. As a consequence, however, the process of mounting the springs to the HDPE base may have inordinately increased the stiffness of the spring by reducing its effective length even further. Therefore, the fixation mechanism and size of the springs selected will need to be reevaluated in future designs.

In addition to complications with the design itself, the testing process is rather involved and requires use of equipment that is limited in availability and high in demand. There are only two neonatal transport isolettes available at the American Family Children's Hospital. Even when testing sessions are scheduled far in advance, if a call is received, these sessions can be canceled with little to no notice as they are needed for emergency transport. As a result, it is difficult to complete testing as frequently as is required to accommodate changes in the design or

testing protocol. For this reason, the following challenges experienced in testing were not able to be corrected for in the course of this semester. The first issue occurred during preliminary testing. Due to an issue with the accelerometer, only half of the 45 minute route was saved. Therefore the baseline data compares a disproportionate amount of time during smoother highway driving relative to the device data and could be falsely undercutting the efficacy of the design. Additionally, during baseline testing, there was not a neonate in the isolette and no mass was placed on top of the tray to mimic the weight of an infant in transport. Given that the calculations for spring constant and damping coefficient were performed under the assumption of a 6 kg mass, the lack of this presence could have diminished its performance.

While there were many potential sources of error this semester, there were also many points that were corrected from previous work on the project. Now having a better understanding of the issues the project encountered in the design process this semester - and the implications of these issues - the team believes there is room for the current design to be improved upon in order to see more desirable results in the future.

VII. Conclusions

Critically-ill neonates are often transported via ambulance or helicopter to hospitals, and the ride could last several hours and undergo various terrain, such as railroad crossings, freeway travel, and stop-and-go traffic. This causes the neonate to experience significant stress due to forces the incubator experiences during transport, ultimately leading to brain damage due to the delicate nature of the neonate during that time. The team was tasked with creating a device that could help to reduce the vibrations that are experienced by a neonate during transport via ambulance or helicopter to a Neonatal Intensive Care Unit (NICU) to lessen the chances of brain injury and to increase the chances of survival.

Prior iterations of prototyping with the Metal and Gel Composite Damper provided a start to solving the problem; however, the results were not significant enough to truly reduce the vibrations enough to positively influence the neonate. Because of this, the team proceeded to follow a different route and chose the Spring and Damper design to continue researching and prototyping in order to solve the task at hand.

The Spring and Damper design consists of four components. Each component consists of three main pieces: a platform, a spring, and a damper. The platform is a 4" x 4" piece of HDPE,

which acts as an attachment mechanism for the spring and a damper. The spring used was the Smalley C0371-L1 crest-to-crest wave spring, with a spring constant of 7880.70 N/m [28]. The damper used was the Sorbothane 40-durometer sheet stock, with a damping coefficient of 1.10 to 1.68 at 10% compression [34]. Both of these materials were chosen based on which most closely matched the calculated values of 7923.1 N/m and 1.25 lbf·sec/in. for the spring and damper, respectively. Three holes were drilled into the HDPE layer, aligning with the three points of contact that the bottom of the spring has to ensure it rests flat. Three pieces of thread were knotted onto the bottom layer of the spring and thread through the holes. One knot was tied tightly to the bottom of the HDPE and coated in a layer of super glue to ensure the knot doesn't come undone or unravel during use. The Sorbothane was cut into 4" x 4" squares with a 1" x 1" section cut out of one corner to ensure the spring wouldn't be covered up. The Sorbothane damping material was stuck onto the HDPE in parallel with the spring.

To integrate this design into the current isolette set up, each of the four components would be placed at one of the four corners of the outer tray, resting in between the inner and outer trays. The exposed adhesive layer of the Sorbothane damping material was secured to the outside bottom of the inner tray to reduce the possibility of undesired movement during use.

The WitMotion WT901SDCL Accelerometer was used to gather acceleration data in the x, y, and z directions. This accelerometer was placed beneath the gel mattress at the general location of where the neonate's head would be. To test this device, the team sat in on two 50 minute ambulance rides that went through railroad tracks, stop-and-go traffic, and freeway travel. The first time on this route was to collect baseline data without the device, and the second time was with the final design placed in the isolette.

The results from these two trials showed promising results. In comparison to last semester's work, the data gathered was slightly different. Last semester's Metal and Gel Composite Damper worked well in shifting the vibration frequencies to a lower frequency overall; however, this semester's Spring and Damper design reduced the vibrations rather than shifting it, which was the desired outcome the team was looking for. The design specifications emphasize the need to reduce vibrations below 0.315 m/s^2 throughout the entire duration of transport, and although the value is not yet reached, the spring and damper design proved to reduce the vibrations throughout the entire frequency range and length of travel, which is why the team will continue to move forward with modifications to this design.

This semester provided several challenges, with the majority being out of the team's control. The most significant challenge was the lack of testing and access to testing due to the limited number of transport isolettes and unknown availability of them. Patients are always the number one priority, so hospital visits were occasionally rescheduled in order to accommodate for that. Despite this hurdle, the fabrication process went relatively seamlessly, which made it easy to spontaneously do testing runs or hospital visits as the team was always prepared for those situations.

Future Work

Although significant progress has been made in the task to reduce vibrations that a neonate experiences during transportation, further research, prototyping, and testing needs to be conducted to see a bigger impact. The team was satisfied with the results from this semester, but the goal of reaching a constant acceleration below 0.315 m/s^2 throughout the whole transport time has not yet been achieved. The first step in reaching this goal will be to modify the materials used. There were several assumptions that were made regarding the properties of the spring constant and damping coefficient, so discussing these with professionals in the field as well as verifying calculations will give the team confidence in the choices of materials. In addition to modifying the spring constant of the spring, a spring with a larger effective length should be used instead of the smaller spring used this semester, as at least one layer of the spring is compromised in the process of securing the spring to the layer of HDPE.

The testing protocol should also be modified in future iterations of testing in order to more accurately simulate the true ride conditions and what is felt by the neonate. This would involve doing testing with a precise mass value and simulating the procedure with a mannequin. Data should be collected at the head of the mannequin to understand the vibrations that the neonate's brain would feel. In addition to improvements in ambulance testing, testing procedures should be established to perform testing with on-campus equipment so that the team is not entirely reliant on isolette availability.

Lastly, this semester's work focused on creating a device that worked primarily in the z-plane as it showed the most significant vibrations during testing. However, it would be ideal to implement a device that operates in both the y and z directions to reduce vibrations in those

directions as well. By addressing these future improvements, the team can further advance the development of a device that effectively reduces vibrations for neonatal transportation.

VIII. References

- [1] “Transport of the Critically Ill Newborn: Overview, Administrative Aspects of Neonatal Transport Services, Neonatal Team Skills.” <https://emedicine.medscape.com/article/978606-overview?reg=1> (accessed Oct. 11, 2022).
- [2] K. Helenius, N. Longford, L. Lehtonen, N. Modi, and C. Gale, “Association of early postnatal transfer and birth outside a tertiary hospital with mortality and severe brain injury in extremely preterm infants: observational cohort study with propensity score matching,” *The BMJ*, vol. 367, p. l5678, Oct. 2019, doi: 10.1136/bmj.l5678.
- [3] A. Synnes *et al.*, “Determinants of developmental outcomes in a very preterm Canadian cohort,” *Arch. Dis. Child. Fetal Neonatal Ed.*, vol. 102, no. 3, pp. F235–F234, May 2017, doi: 10.1136/archdischild-2016-311228.
- [4] R. A. Boland, P. G. Davis, J. A. Dawson, and L. W. Doyle, “Outcomes of infants born at 22-27 weeks’ gestation in Victoria according to outborn/inborn birth status,” *Arch. Dis. Child. Fetal Neonatal Ed.*, vol. 102, no. 2, pp. F153–F161, Mar. 2017, doi: 10.1136/archdischild-2015-310313.
- [5] “Preterm birth.” <https://www.who.int/news-room/fact-sheets/detail/preterm-birth> (accessed Oct. 11, 2022).
- [6] “Recent trends in hospital use by children in England | Archives of Disease in Childhood.” <https://adc.bmj.com/content/85/3/203.long> (accessed Oct. 11, 2022).
- [7] S. Kempley, A. Sinha, and b on, “Census of neonatal transfers in London and the South East of England,” *Arch. Dis. Child. Fetal Neonatal Ed.*, vol. 89, no. 6, pp. F521–F526, Nov. 2004, doi: 10.1136/adc.2003.029017.
- [8] American Academy of Pediatrics and American College of Obstetricians and Gynecologists, Eds., *Guidelines for perinatal care*, 7th ed. Elk Grove Village, IL : Washington, DC: American Academy of Pediatrics ; American College of Obstetricians and Gynecologists, 2012.
- [9] M. I. Levene, C. L. Fawer, and R. F. Lamont, “Risk factors in the development of intraventricular haemorrhage in the preterm neonate.,” *Arch. Dis. Child.*, vol. 57, no. 6, pp. 410–417, Jun. 1982.
- [10] K. Derry, “C-06-12-60558 Infant Securement On Neonatal Transport In Transport Incubator,” p. 4.
- [11] 14:00-17:00, “ISO 2631-5:2018,” *ISO*. <https://www.iso.org/standard/50905.html> (accessed Feb. 06, 2023).
- [12] J. Zhou, K. Wang, D. Xu, H. Ouyang, and Y. Fu, “Vibration isolation in neonatal transport by using a quasi-zero-stiffness isolator,” *J. Vib. Control*, vol. 24, no. 15, pp. 3278–3291, Aug. 2018, doi: 10.1177/1077546317703866.
- [13] M. Bailey-vankuren and A. Shukla, “Isolation device for shock reduction in a neonatal transport apparatus,” 20070089236, Apr. 26, 2007 Accessed: Sep. 22, 2022. [Online]. Available: <https://www.freepatentsonline.com/y2007/0089236.html>
- [14] J. Lopes, K. Leuraud, D. Klokov, C. Durand, M.-O. Bernier, and C. Baudin, “Risk of Developing Non-Cancerous Central Nervous System Diseases Due to Ionizing Radiation Exposure during Adulthood: Systematic Review and Meta-Analyses,” *Brain Sci.*, vol. 12, no. 8, Art. no. 8, Aug. 2022, doi: 10.3390/brainsci12080984.
- [15] P. Ballabh, “Intraventricular Hemorrhage in Premature Infants: Mechanism of Disease,” *Pediatr. Res.*, vol. 67, no. 1, pp. 1–8, Jan. 2010, doi: 10.1203/PDR.0b013e3181c1b176.
- [16] I. Goswami, “Whole-body vibration in neonatal transport: a review of current knowledge and future research challenges - ClinicalKey.” <https://www-clinicalkey-com.ezproxy.library.wisc.edu/#!/content/playContent/1-s2.0-S0378378220302139?returnurl=null&referrer=null> (accessed Sep. 21, 2022).
- [17] “AboutKidsHealth.” <https://www.aboutkidshealth.ca:443/article?contentid=1810&language=english> (accessed Dec. 14, 2022).
- [18] “Voyager – int-bio.” <https://int-bio.com/neonatal-transport/transport-incubators/voyager/> (accessed Oct. 12, 2022).

- [19] B. Biju, A. Ramesh, A. R. Krishnan, A. G. Nath, and C. J. Francis, "Damping characteristics of woodpecker inspired layered shock absorbing structures," *Mater. Today Proc.*, vol. 25, pp. 140–143, Jan. 2020, doi: 10.1016/j.matpr.2019.12.187.
- [20] S.-H. Yoon and S. Park, "A mechanical analysis of woodpecker drumming and its application to shock-absorbing systems," *Bioinspir. Biomim.*, vol. 6, no. 1, p. 016003, Jan. 2011, doi: 10.1088/1748-3182/6/1/016003.
- [21] "Seismic performance evaluation of a spring viscous damper cable system | Elsevier Enhanced Reader." <https://reader.elsevier.com/reader/sd/pii/S0141029618309738?token=8CDA639C645DD8438638D7E612D1E80ACD5912ECE5151D7FDC0A5446BA70244719CA362E705A8B1F41762B1840F15A77&originRegion=us-east-1&originCreation=20230214025651> (accessed Feb. 13, 2023).
- [22] D. De Domenico, G. Ricciardi, and I. Takewaki, "Design strategies of viscous dampers for seismic protection of building structures: A review," *Soil Dyn. Earthq. Eng.*, vol. 118, pp. 144–165, Mar. 2019, doi: 10.1016/j.soildyn.2018.12.024.
- [23] "Vibrating Systems." https://ccrma.stanford.edu/CCRMA/Courses/152/vibrating_systems.html (accessed Feb. 27, 2023).
- [24] T. Aoki, Y. Yamashita, and D. Tsubakino, "Vibration Suppression of Mass-Spring-Damper System with Dynamic Dampers using IDA-PBC* *This research is partially supported by a JSPS Grant-in-Aid for Scientific Research (B) (22360167).," *IFAC Proc. Vol.*, vol. 45, no. 19, pp. 42–47, Jan. 2012, doi: 10.3182/20120829-3-IT-4022.00021.
- [25] "Damper Spring | 3D CAD Model Library | GrabCAD." <https://grabcad.com/library/damper-spring-1> (accessed Feb. 14, 2023).
- [26] "How Car Suspensions Work," *HowStuffWorks*, May 11, 2005. <https://auto.howstuffworks.com/car-suspension.htm> (accessed Feb. 28, 2023).
- [27] admin, "Wave Springs," *Smalley*, Dec. 23, 2013. <https://www.smalley.com/wave-springs> (accessed Feb. 25, 2023).
- [28] admin, "C037-L1," *Smalley*, Oct. 03, 2013. <https://www.smalley.com/wave-spring/c037-l1> (accessed Apr. 19, 2023).
- [29] F. Fronczak, *Forced Vibration: Systems with a Single Degree of Freedom*, 1st ed.
- [30] "What is a Power Spectral Density (PSD)?" <https://community.sw.siemens.com/s/article/what-is-a-power-spectral-density-psd> (accessed Feb. 28, 2023).
- [31] A. Avasthi, A. Ghosh, S. Sarkar, and S. Grover, "Ethics in medical research: General principles with special reference to psychiatry research," *Indian J. Psychiatry*, vol. 55, no. 1, pp. 86–91, Mar. 2013, doi: 10.4103/0019-5545.105525.
- [32] C. for D. and R. Health, "Classify Your Medical Device," *FDA*, Oct. 22, 2020. <https://www.fda.gov/medical-devices/overview-device-regulation/classify-your-medical-device> (accessed Dec. 14, 2022).
- [33] C. for D. and R. Health, "Sterilization for Medical Devices," *FDA*, Sep. 2022, Accessed: Sep. 21, 2022. [Online]. Available: <https://www.fda.gov/medical-devices/general-hospital-devices-and-supplies/sterilization-medical-devices>
- [34] R. Pope, "Vibration Damping Material," *Sorbothane*, Jan. 31, 2015. <https://www.sorbothane.com/technical-data/articles/vibration-damping-material/> (accessed Feb. 12, 2023).

IX. Appendix

A. Product Design Specifications

Product Design Specification

Reducing Whole-Body Vibrations in Neonatal Transport

Feb 10, 2023

Team Members:	Joshua Varghese	Team Leader
	Meghan Horan	Communicator
	Sydney Polzin	BWIG
	Joseph Byrne	BPAG
	Nicole Parmenter	BSAC

Function:

Critically ill neonates, as a result of birth defects or other disorders, require transport to neonatal intensive care units (NICU) where specialized medical professionals and equipment increase their chances of survival. Transport in ambulances or helicopters, while necessary, induces physiological stressors which adversely affect the health of the neonates. In particular, whole body vibration (WBV) and excessive sound levels can induce head bleeds, leading to subsequent neurodevelopmental impairment or death. Minimizing the effects of mechanical vibrations and rotational and translational motion could improve outcomes during transport. The current transport incubator has ventilators, monitoring equipment, and temperature control mechanisms, but no control of the physical stressors aforementioned. The client, Dr. Ryan McAdams, tasked the team with developing a novel transport bed to minimize these issues. The new bed must ensure the safety and security of the neonate while maintaining the functions of current incubators.

Client requirements:

1. The device must minimize the vibrational forces within the incubator so that a critical neonate does not sustain injury.
2. The device must minimize translational and rotational forces enough to prevent injury to critical neonates.
3. The device must either attach to current incubators or include all the associated functions including ventilators, monitoring equipment, and temperature control mechanisms.
4. The device must be small enough to fit within a standard ambulance and allow the movement of the transport team.
5. The data collection method must meet industry standards and provide appropriate support to justify the damper design's effectiveness at reducing whole body vibrations.

Design requirements:**1) Physical and Operational Characteristics***a) Performance requirements*

- i) The product must decrease the amount of whole-body vibrations to be below 0.315 m/s^2 as suggested by ISO standard 2631 regarding human exposure to whole-body vibrations [1].
- ii) The product should allow the infant to maintain proper vital signs in a range appropriate for its size, age, and condition:
 - (1) A heart rate between 100 and 160 beats per minute [2].
 - (2) A respiratory rate between 30 and 60 breaths per minute [2].
 - (3) Blood pressure of no less than 30 mmHg systolic [3].
 - (4) An oxygen saturation level between 85% and 95% [4].
- iii) The sampling frequency of the testing mechanism should be at least 100 Hz in order to appropriately cover the range of frequencies experienced within the incubator while traveling in an ambulance or helicopter [5].
- iv) The testing mechanism should be able to continuously collect and store data for at least 1 week.

b) Safety

- i) The transport bed, and any alterations made to it, must not inhibit the delivery of continuous treatment to the neonate.
- ii) The device should not interrupt the functioning of the incubator, ventilator, or monitoring equipment.
- iii) Any potentially hazardous components of the device (e.g. sharp edges, long cords, or small pieces) should not be accessible to the neonate while in the incubator.
- iv) The device should be able to be decontaminated with a U.S. Environmental Protection Agency (EPA)-registered hospital disinfectant without degradation for the 5 year lifetime of the ambulance [6].

c) Accuracy and Reliability

- i) The device should be able to effectively reduce the amplitude of vibrations with a frequency in the human sensitivity range of 3-20 Hz [7].
- ii) The root mean square vibration exposure should fall below the 0.315 m/s^2 comfort limit specified in ISO 2631 [1].
- iii) The device should not lose function or require maintenance over the course of its lifespan.
- iv) The device should be functional when supporting neonates from 2.5-4.5 kilograms [8].

d) Life in Service

- i) On average, ambulances have a lifespan of around 5 years and travel around 300,000 miles, assuming proper maintenance and standard operating conditions. The device should be able to withstand these conditions [9].
- ii) Incubators can last several years, but undergo significant stress due the vibrations and mechanical forces they withstand on a day-to-day basis and due to intense transportation (e.g., ambulance rides, cleaning, etc.). The device should be able to withstand similar mechanical stress to the incubator and last around a similar time frame [10].
- iii) The device should not compromise the functionality or safety of the incubator throughout the lifespan of its use.

e) Shelf Life

- i) If electrical components are involved in the design, the device should function for a minimum of 7 years [11].
- ii) If no electrical components are included, the device should last for at least 12 years [11].

f) Operating Environment

- i) The operating environment for both the dampening device and testing mechanism will be targeted for ground transport using an ambulance and the Voyager transport incubator by International Biomedical [12].

g) Ergonomics

- i) No parts of the device will interfere with ambulance personnel or obstruct access to the neonate.
- ii) For any electrical components, there will be a simple screen interface.

h) Size

- i) The device will fit inside or under the Voyager transport incubator by International Biomedical with dimensions of 53 cm H x 48 cm W x 99 cm L [13].

i) Weight

- i) The dampening device should be no more than 4 kg which is equivalent to 10% of the incubator's weight when empty [13].
- ii) The testing mechanism should contribute less than 2 kg to the incubator system so that its weight will have a minimal effect on the vibrations experienced by the neonate [14].

j) Materials

- i) The materials should be safe to use in a medical environment and be in compliance with federal EMS regulations [12].
- ii) The damping device and testing mechanism should avoid using heavy metals or latex materials on portions of the device that may come into contact with a patient [15].

k) *Aesthetics, Appearance, and Finish*

- i) The device should appear as a part of the incubator, but with distinguishing characteristics, such as color or material, that set it apart from the incubator as a whole. This will assist in removal, isolation, and cleaning of the device if needed.
- ii) The color of the device should be either white, green, or blue, which all symbolize cleanliness. Color selection is important to provide confidence to the client and user that the product was professionally developed and is functional [16].
- iii) Appearance and material considerations and choices should not ultimately affect the functionality of the device. FDA regulations surrounding material and color choices need to be carefully considered.

2) Production Characteristics

a) *Quantity*

- i) A single functional prototype should be developed by the conclusion of the semester.
- ii) A single testing device must be acquired to perform repeat testing on both the initial prototype and future developments.
- iii) Design should be able to be mass produced for commercial use in the future.

b) *Target Product Cost*

- i) The design should cost no more than \$500 for preliminary development and testing.

3) Miscellaneous

a) *Standards and Specifications*

- i) The dampening prototype can be considered a Class I or Class II device depending on the modifications that accompany the design. Either class will require compliance with sections 513(a)(1)(A)- general controls, 513(a)(1)(B)- special controls and specific risks, and potentially 510(k)- premarket notification [17].
 - (1) If the device modifies the incubator and replaces any components that are present in International Biomedical's Voyager, then it will require FDA approval and must meet requirements for a class II medical device
 - (2) If the device does not alter the incubator setup and presents a minimal risk to the patient, then it may meet the requirements described for class I devices.
- ii) To ensure safety and efficacy, the device must follow the requirements under 21 CFR Part 820- Quality System Regulation [18].

- iii) The device must comply with sterilization standards described in ISO 14937 [19].
- iv) If the device directly alters the isolette, it must meet the standards in IEC 60601-2-20, which outlines safety and performance requirements for transport incubators [20].

b) Customer

- i) The hospital requesting the device requires that the device is compatible with their preexisting transport setup.
 - (1) Alternatively, the design should include all the associated functions of a transport incubator including temperature control, ventilators, and monitoring systems.
- ii) The design should fit within a standard ambulance and not hinder the mobility of transport teams.
 - (1) The maximum area for device implementation, as detailed for Type III Transport Ambulances, is 173 cm interior headroom and 124 cm aisle width [21]. It is important to note these are maximum size constraints while the functional design area may be limited further within this space for mobility and accessibility.
- iii) The design must improve transport outcomes by reducing vibrations with no additional adverse effects on patient health.

c) Patient-related concerns

- i) During use and transport, the device should not introduce any additional threats or risks to the neonate.
- ii) The product should not come in contact with the patient in case of allergic reaction to the material.
- iii) Thorough testing must be completed before testing on patients can occur to ensure comfortability, safety, and effectiveness. All risk management procedures must be fully and carefully analyzed.

d) Competition

- i) The Quasi-Zero-Stiffness (QZS) Isolator is a proposed design which targets low-frequency vibrations via modifications made to the incubator control box [22]. The design primarily utilizes concentric magnets and coil springs to mitigate vibrations. However, the design requires extensive modifications to the preexisting setup and has not been experimentally proven.
- ii) The isolation device for shock reduction is another proposed design which utilizes gas springs between the isolette and stretcher deck [23]. The design features variable pressures in the springs as a way to target various frequency ranges. The proposed design makes considerable modifications to the preexisting setup while failing to acknowledge the presence of monitoring systems.

- iii) Magnetorheological (MR) dampers help stop vibrations in vehicles when driving on roads that have changes in smoothness and shape. The pneumatic suspension system can be set to be soft or firm, and the MR damper can be adjusted to different levels of firmness to work with the pneumatic suspension and reduce vibrations [24].

References:

- [1] 14:00-17:00, “ISO 2631-5:2018,” *ISO*. <https://www.iso.org/standard/50905.html> (accessed Feb. 06, 2023).
- [2] S. Reuter, C. Moser, and M. Baack, “Respiratory Distress in the Newborn,” *Pediatr. Rev.*, vol. 35, no. 10, pp. 417–429, Oct. 2014.
- [3] “Blood pressure disorders | Safer Care Victoria.” <https://www.safercare.vic.gov.au/clinical-guidance/neonatal/blood-pressure-disorders> (accessed Feb. 06, 2023).
- [4] American Academy of Pediatrics and American College of Obstetricians and Gynecologists, Eds., *Guidelines for perinatal care*, Eighth edition. Elk Grove Village, IL : Washington, DC: American Academy of Pediatrics ; The American College of Obstetricians and Gynecologists, 2017.
- [5] I. Goswami, “Whole-body vibration in neonatal transport: a review of current knowledge and future research challenges - ClinicalKey.” <https://www-clinicalkey-com.ezproxy.library.wisc.edu/#!/content/playContent/1-s2.0-S0378378220302139?returnurl=null&referrer=null> (accessed Sep. 21, 2022).
- [6] “Example: Standard Operating Procedure (SOP) for Decontamination of an Ambulance that has Transported a Person under Investigation or Patient with Confirmed Ebola | Emergency Services | Clinicians | Ebola (Ebola Virus Disease) | CDC,” May 06, 2019. <https://www.cdc.gov/vhf/ebola/clinicians/emergency-services/ambulance-decontamination.html> (accessed Feb. 06, 2023).
- [7] L. Blaxter *et al.*, “Neonatal head and torso vibration exposure during inter-hospital transfer,” *Proc. Inst. Mech. Eng. [H]*, vol. 231, no. 2, pp. 99–113, Feb. 2017, doi: 10.1177/0954411916680235.
- [8] K. Shehzad, “Neonatal birth-weights and reference intervals in sonographically monitored normal fetuses,” *Int. J. Health Sci.*, vol. 5, no. 2 Suppl 1, p. 27, Jul. 2011.
- [9] “Ambulance Replacement,” *CCMH Foundation*. <https://www.ccmhgiving.com/ambulance-replacement/> (accessed Feb. 07, 2023).
- [10] V. DeFrancesco, “93 - Perinatology,” in *Clinical Engineering Handbook*, J. F. Dyro, Ed. Burlington: Academic Press, 2004, pp. 410–416. doi: 10.1016/B978-012226570-9/50102-2.
- [11] S. Loznen, “Expected Service Life of Medical Electrical Equipment,” *In Compliance Magazine*, Oct. 29, 2021. <https://incompliancemag.com/article/expected-service-life-of-medical-electrical-equipment/> (accessed Feb. 05, 2023).
- [12] H. H. de Anda and H. P. Moy, “EMS Ground Transport Safety,” in *StatPearls*, Treasure Island (FL): StatPearls Publishing, 2022. Accessed: Feb. 06, 2023. [Online]. Available: <http://www.ncbi.nlm.nih.gov/books/NBK558971/>
- [13] “Voyager – int-bio.” <https://int-bio.com/neonatal-transport/transport-incubators/voyager/> (accessed Feb. 05, 2023).
- [14] Y.-Z. Jiang, K.-F. He, Y.-L. Dong, D. Yang, and W. Sun, “Influence of Load Weight on Dynamic Response of Vibrating Screen,” *Shock Vib.*, vol. 2019, p. e4232730, Apr. 2019, doi: 10.1155/2019/4232730.
- [15] C. for D. and R. Health, “Safety of Metals and Other Materials Used in Medical Devices,” *FDA*, Feb. 2022, Accessed: Feb. 07, 2023. [Online]. Available: <https://www.fda.gov/medical-devices/products-and-medical-procedures/safety-metals-and-other-materials-used-medical-devices>
- [16] “The role of colour in medical devices: a designer’s perspective | Team Consulting.” <https://www.team-consulting.com/insights/the-role-of-colour-in-medical-devices-a-designers-perspective/> (accessed Feb. 07, 2023).
- [17] C. for D. and R. Health, “Classify Your Medical Device,” *FDA*, Oct. 22, 2020. <https://www.fda.gov/medical-devices/overview-device-regulation/classify-your-medical-device> (accessed Feb. 07, 2023).
- [18] “21 CFR Part 820 -- Quality System Regulation.” <https://www.ecfr.gov/current/title-21/chapter-I/subchapter-H/part-820> (accessed Feb. 07, 2023).
- [19] “ISO 14937:2009(en), Sterilization of health care products — General requirements for

- characterization of a sterilizing agent and the development, validation and routine control of a sterilization process for medical devices.” <https://www.iso.org/obp/ui/#iso:std:iso:14937:ed-2:v1:en> (accessed Feb. 07, 2023).
- [20] “IEC 60601-2-20:2020 RLV | IEC Webstore.” <https://webstore.iec.ch/publication/67567> (accessed Feb. 07, 2023).
- [21] “Osage-Type-Warrior-III-Ford-E350-Drawings.pdf.” Accessed: Feb. 07, 2023. [Online]. Available: <https://www.bulldogfireapparatus.com/wp-content/uploads/2020/07/Osage-Type-Warrior-III-Ford-E350-Drawings.pdf>
- [22] J. Zhou, K. Wang, D. Xu, H. Ouyang, and Y. Fu, “Vibration isolation in neonatal transport by using a quasi-zero-stiffness isolator,” *J. Vib. Control*, vol. 24, no. 15, pp. 3278–3291, Aug. 2018, doi: 10.1177/1077546317703866.
- [23] M. Bailey-vankuren and A. Shukla, “Isolation device for shock reduction in a neonatal transport apparatus,” 20070089236, Apr. 26, 2007 Accessed: Sep. 22, 2022. [Online]. Available: <https://www.freepatentsonline.com/y2007/0089236.html>
- [24] A. L. Morales, A. J. Nieto, J. M. Chicharro, and P. Pintado, “A semi-active vehicle suspension based on pneumatic springs and magnetorheological dampers,” *J. Vib. Control*, vol. 24, no. 4, pp. 808–821, Feb. 2018, doi: 10.1177/1077546316653004.

B. Testing Results from Fall 2022 Prototype

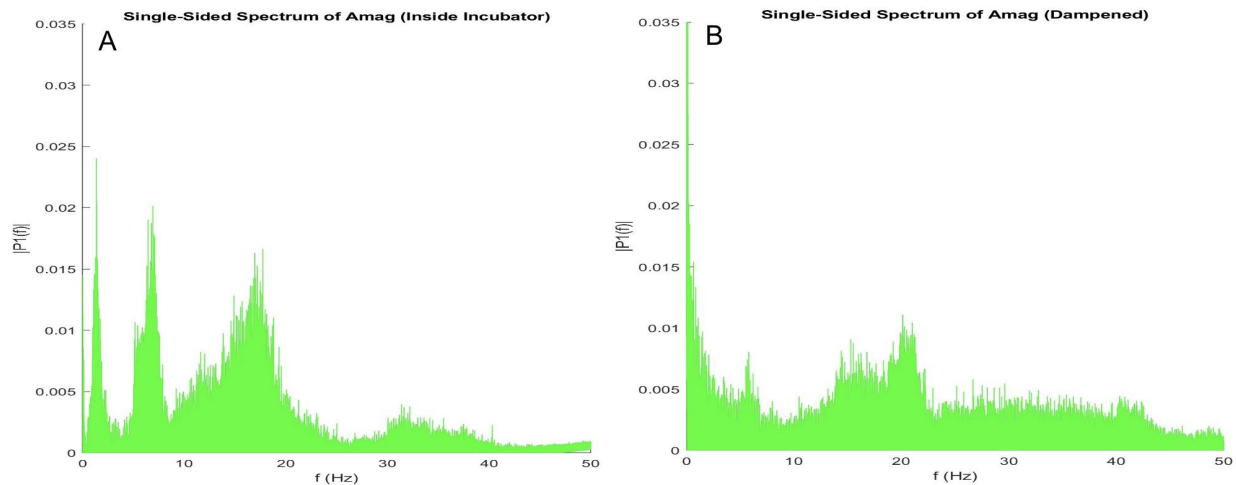


Figure 1: Power spectral density graphs for measurements (A) inside the incubator without the dampening prototype, and (B) inside the incubator with the dampening prototype.

The acceleration data acquired from the testing runs was uploaded to MATLAB drive. A Discrete Fourier Transformation was applied to the total magnitude of the acceleration data to gather the frequency information. An analysis of the frequency derived from the transform was done to provide information about the vibrations experienced by the neonate mannequin inside the isolette as well as the surrounding setup. The data was cleaned using the detrend function in MATLAB to remove the best straight-fit line. The sensors were grouped by location for analysis; the two sensors inside the incubator during undamped baseline testing were grouped together, and the two sensors inside the incubator during dampened device testing were grouped together. These groups were formed so that performance of the damper could be compared to vibrations experienced inside and outside the incubator during a standard transport trip. Power spectral density graphs were created for each of the three sensor groupings in Figure 1. Qualitative size comparison of the spectrums in Figure 1 (A) and (B) from baseline testing suggests that a large amplification of vibrations occurs inside the incubator within the 0 to 20 Hz range.

C. Fabrication Methods

After obtaining materials, the spring damper combinations were fabricated and inserted between the inner and outer trays of the isolette according to the following steps.

1. Four 4" x 4" squares of 1/8" thick HDPE plastic and four 4" x 4" squares of Sorbothane® viscoelastic polymer (1/10"- 40-DURO-Black Sheet) acting as the damping material were cut out.
2. One 1" x 1" square was cut out of one corner of each 4" x 4" Sorbothane® square to provide a surface to attach the spring.
3. The Sorbothane® pieces were already adhesive and were stuck to the HDPE bases.
4. One Smalley® carbon steel, flat wire spring was attached to each of the four HDPE base pieces.
 - a. The spring has three points of contact with the surface it sits on. The spring was measured and three holes were drilled with a 7/64-in drill bit into the corner of the HDPE where the Sorbothane® was cut out corresponding to these contact points.
 - b. Thread was looped through the bottom of the spring and the holes in the HDPE base to hold the springs in place. A knot was tied under the base and super glued in place to prevent movement, fraying, and slippage.
5. The spring damper combinations were inserted between the inner and outer trays of the isolette.
 - a. One spring damper combination was placed in each corner of the outer tray.
 - b. The spring was located in the corner closest to the corner of the tray it resided in.
 - c. The adhesive side of the Sorbothane® that was not stuck to the HDPE base was stuck to the bottom of the inner tray to prevent sliding of the prototype during transport.

D. Spring & Damper Calculations

Known Values: m , $\omega_{\text{excitation}}$, & ω/ω_n

Needed Values: k & c

m is the mass that is oscillating. In this case, it is the combined mass of the neonate, tray, mattress, and involved equipment treated as a point mass.

The $\omega_{\text{excitation}}$ value will be the 17 Hz frequency (from Fall 2022 testing) multiplied by 2π .

ω/ω_n can be found once you have determined a displacement (Y/X) and a ζ value. We assume both to be ~ 0.2 . For displacement, this means that the amplitude of vibrations is approximately 20% of their original magnitude. For ζ , 0.2 is chosen as it shows a termination of oscillation after approximately 2 cycles (as illustrated in **Figure 1**). However, these values are based on judgment and may need to be optimized.

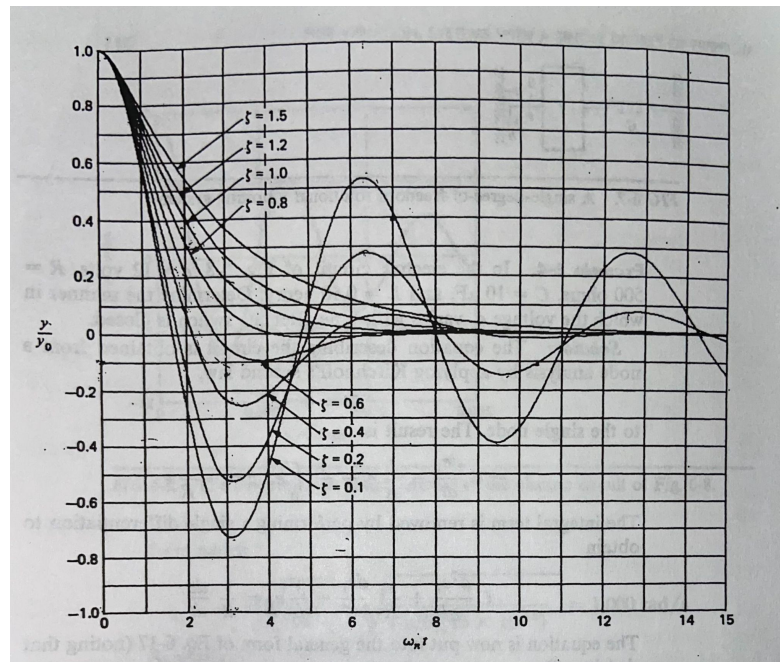


Figure 1: Free-vibration characteristics of a single-degree-of-freedom mass-spring-damper system and other dynamic second-order systems

With these two values selected, the displacement transmissibility plot (**Figure 2**) can be used to determine the value of ω/ω_n and it turns out to be ~ 3

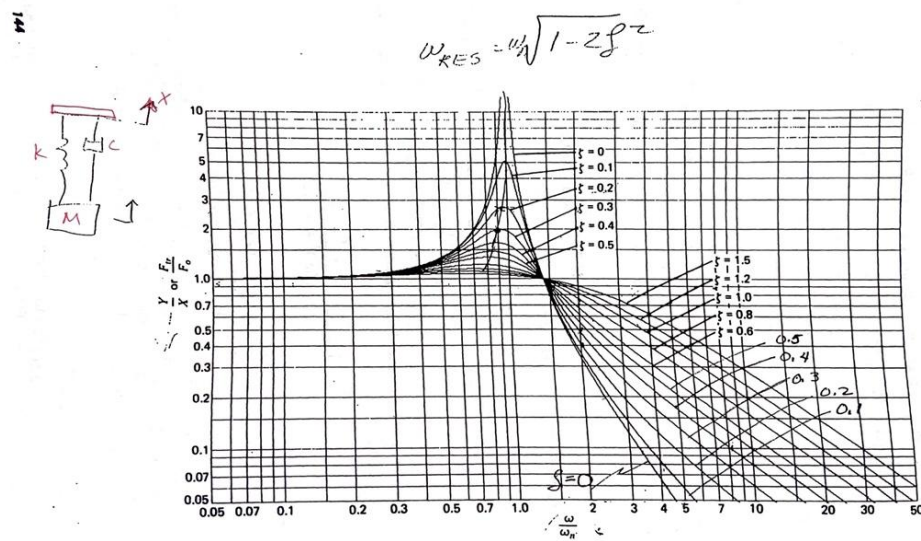


Figure 2: Displacement transmissibility plot

Once ω , ω_n and $\omega_{excitation}$ are known, ω_n can be calculated.

$\omega_n = \sqrt{k/m}$ -- solve for k , the spring constant

$$C_{critical} = \sqrt{4mk}$$

Knowing $C_{critical}$ and ζ , find the damping coefficient, c

$$\zeta = \frac{C_{critical}}{c}$$

E. Sorbothane Damping Coefficients

30 Durometer			
Specified Frequency Hz	C lbf-Sec/in		
	10% Compression	15% Compression	20% Compression
1	5.33	6.08	7.15
5	2.22	2.55	3.00
15	1.22	1.40	1.65
30	0.83	0.95	1.12
50	0.62	0.71	0.84
75	0.49	0.56	0.65
100	0.41	0.47	0.54
125	0.36	0.41	0.47
150	0.32	0.36	0.42
175	0.29	0.33	0.38
200	0.27	0.31	0.34
225	0.24	0.28	0.32
250	0.23	0.26	0.29
275	0.21	0.24	0.28
300	0.20	0.23	0.26

40 Durometer			
Specified Frequency Hz	C lbf-Sec/in		
	10% Compression	15% Compression	20% Compression
1	7.97	9.34	10.69
5	3.19	3.67	4.22
15	1.68	1.92	2.21
30	1.10	1.26	1.45
50	0.81	0.92	1.06
75	0.62	0.71	0.81
100	0.52	0.59	0.67
125	0.44	0.50	0.57
150	0.40	0.45	0.51
175	0.35	0.40	0.45
200	0.32	0.36	0.41
225	0.30	0.34	0.37
250	0.27	0.30	0.34
275	0.26	0.28	0.32
300	0.24	0.26	0.30

50 Durometer			
Specified Frequency Hz	C lbf-Sec/in		
	10% Compression	15% Compression	20% Compression
1	10.19	11.61	14.01
5	4.00	4.55	5.43
15	2.09	2.37	2.80
30	1.37	1.56	1.84
50	1.00	1.13	1.32
75	0.76	0.87	0.99
100	0.64	0.72	0.81
125	0.55	0.62	0.69
150	0.49	0.54	0.59
175	0.43	0.49	0.53
200	0.40	0.43	0.47
225	0.36	0.39	0.43
250	0.33	0.36	0.40
275	0.31	0.34	0.36
300	0.29	0.31	0.34

60 Durometer			
Specified Frequency Hz	C lbf-Sec/in		
	10% Compression	15% Compression	20% Compression
1	11.14	12.78	15.21
5	4.08	4.72	5.61
15	2.02	2.33	2.78
30	1.28	1.48	1.76
50	0.89	1.03	1.24
75	0.68	0.78	0.93
100	0.55	0.63	0.74
125	0.47	0.54	0.62
150	0.42	0.48	0.54
175	0.37	0.43	0.50
200	0.33	0.39	0.45
225	0.30	0.35	0.40
250	0.28	0.33	0.37
275	0.26	0.31	0.34
300	0.25	0.28	0.32

70 Durometer			
Specified Frequency Hz	C lbf-Sec/in		
	10% Compression	15% Compression	20% Compression
1	14.79	16.50	19.11
5	5.25	5.89	6.79
15	2.52	2.82	3.26
30	1.57	1.76	2.03
50	1.10	1.22	1.40
75	0.82	0.91	1.05
100	0.67	0.74	0.84
125	0.56	0.63	0.71
150	0.49	0.54	0.62
175	0.44	0.47	0.55
200	0.39	0.43	0.49
225	0.36	0.39	0.44
250	0.33	0.36	0.40
275	0.30	0.33	0.36
300	0.28	0.31	0.33

80 Durometer			
Specified Frequency Hz	C lbf-Sec/in		
	10% Compression	15% Compression	20% Compression
1	15.35	17.84	21.37
5	5.32	6.25	7.42
15	2.50	2.94	3.50
30	1.53	1.81	2.15
50	1.04	1.24	1.46
75	0.79	0.92	1.08
100	0.63	0.73	0.85
125	0.54	0.60	0.68
150	0.46	0.53	0.61
175	0.42	0.48	0.56
200	0.37	0.43	0.49
225	0.33	0.38	0.44
250	0.31	0.35	0.41
275	0.28	0.33	0.36
300	0.26	0.30	0.34

Figure 1: Tables of Sorbothane® damping coefficients.

F. Expenses and Purchases

Table 1: Purchases made during Spring 2023 semester.

Item	Description	Manufacturer	Mft Pt#	Vendor	Vendor Cat#	Date	QTY	Cost Each	Total	Link
Component 1 (Accelerometer)										
9-Axis Accelerometer	Measures vibrations in the incubator during transport.	Wit Motion	WT901mpu9250	Amazon	B083R3Q5K8	3/17/2023	1	\$53.99	\$53.99	Accelerometer
Component 2 (Other)										
FOCHEW Portable Charger	External Battery Pack for charging accelerometer during testing.	FOCHEW		Amazon	B0BCQKB67J	3/17/2023	1	\$29.95	\$29.95	Charger
								TOTAL:	\$83.94	

G. MATLAB Code

```

clear all;

close all;

filename_f = "FinalData.txt";
fid_f = importdata(filename_f, '\t');
data_f = fid_f;

% Convert the time strings to datetime format
start_time_f = datetime(data_f.textdata(3:end,3), 'InputFormat', 'yyyy-MM-dd HH:mm:ss.SSS');
time_f = datetime(data_f.textdata(3:end,2), 'InputFormat', 'HH:mm:ss.SSS');
time_f = time_f(1620:end);

% Calculate the time elapsed since the start of the recording
time_elapsed_f = seconds(start_time_f - min(start_time_f));

acc_x_f = data_f.data(:, 1);

% Find indices of NaN values
nan_idx_f = find(isnan(acc_x_f));

% Replace NaN values with average of values before and after
for i = nan_idx_f
    acc_x_f(i) = (acc_x_f(i-1) + acc_x_f(i+1)) / 2;
end

acc_y_f = data_f.data(:, 2);

% Find indices of NaN values
nan_idx_f = find(isnan(acc_y_f));

% Replace NaN values with average of values before and after
for i = nan_idx_f
    acc_y_f(i) = (acc_y_f(i-1) + acc_y_f(i+1)) / 2;
end

acc_z_f = data_f.data(:, 3);

% Find indices of NaN values
nan_idx_f = find(isnan(acc_z_f));

% Replace NaN values with average of values before and after
for i = nan_idx_f
    acc_z_f(i) = (acc_z_f(i-1) + acc_z_f(i+1)) / 2;
end

acc_x_f = detrend(acc_x_f(1620:end));
acc_y_f = detrend(acc_y_f(1620:end));
acc_z_f = detrend(acc_z_f*9.8-9.8);
%acc_z_f = detrend(acc_z_f(1620:16340));

L = length(acc_z_f); % Length of signal
Fs = 200; % Sampling frequency
T = 1/Fs; % Sampling period
t = (0:L-1)*T; % Time vector

% plot raw z direction acceleration
plot(t*20, acc_z_f, 'r')

title("Acceleration in Z-direction with Prototype")

```

```

ylim([-10 10])
xlim([0 3300])
xlabel("Time (s)")
ylabel("Acceleration (m/s^2)")
fprintf('%0.2f%% of values in acc_z_f are greater than %0.3f\n', 100*sum(acc_z_f > 0.315)/numel(acc_z_f), 0.315);
fft_A = fft(acc_z_f');
P2 = abs(fft_A/L);
P4 = P2(1:L/2+1);
P4(2:end-1) = 2*P4(2:end-1);
f = Fs*(0:(L/2))/L;
figure(1)
plot(f,P4)
title("Final Single-Sided Amplitude Spectrum of Acceleration in Z-direction")
xlabel("f (Hz)")
ylabel("|P1(f)|")
ylim([0,0.1])
% Set parameters for pwelch function
window = hann(1024); % Window function for spectral analysis
noverlap = 4; % Number of samples to overlap between adjacent windows
% Compute the PSD of the acceleration data
[Pzz_f, f] = pwelch(acc_z_f, window, noverlap, [], Fs);
% Plot the PSD
plot(f, log(Pzz_f)); % Use log-log scale for both axes
xlabel('Frequency (Hz)');
ylabel('Power/Frequency (dB/Hz)');
title('Final Power Spectral Density of Z-Acceleration Data');
grid on;

```

```

filename_i = "PrelimData.txt";
fid_i = importdata(filename_i, '\t');
data_i = fid_i;
% Convert the time strings to datetime format
start_time_i = datetime(data_i.textdata(3:end,3), 'InputFormat', 'yyyy-MM-dd HH:mm:ss.SSS');
time_i = datetime(data_i.textdata(3:end,2), 'InputFormat', 'HH:mm:ss.SSS');
time_i = time_i(2980:18069);
% Calculate the time elapsed since the start of the recording
time_elapsed_i = seconds(start_time_i - min(start_time_i));
acc_x_i = data_i.data(:, 1);
% Find indices of NaN values
nan_idx_i = find(isnan(acc_x_i));
% Replace NaN values with average of values before and after
for i = nan_idx_i
acc_x_i(i) = (acc_x_i(i-1) + acc_x_i(i+1)) / 2;
end
acc_y_i = data_i.data(:, 2);
% Find indices of NaN values

```

```

nan_idx_i = find(isnan(acc_y_i));

% Replace NaN values with average of values before and after
for i = nan_idx_i
acc_y_i(i) = (acc_y_i(i-1) + acc_y_i(i+1)) / 2;
end

acc_z_i = data_i.data(:, 3);

% Find indices of NaN values
nan_idx_i = find(isnan(acc_z_i));

% Replace NaN values with average of values before and after
for i = nan_idx_i
acc_z_i(i) = (acc_z_i(i-1) + acc_z_i(i+1)) / 2;
end

acc_x_i = detrend(acc_x_i(2980:18069))
acc_y_i = detrend(acc_y_i(2980:18069))
acc_z_i = acc_z_i*9.8-9.8;
acc_z_i = detrend(acc_z_i(2980:17700))

L = length(acc_z_i); % Length of signal
Fs = 200; % Sampling frequency
T = 1/Fs; % Sampling period
t = (0:L-1)*T; % Time vector

% plot raw z direction acceleration
plot(t*20, acc_z_i, 'g')

title("Acceleration in Z-direction Without Prototype")

ylim([-10 10])

xlabel("Time (s)")

ylabel("Acceleration (m/s^2)")

fprintf('%0.2f%% of values in acc_z_i are greater than %0.3f\n', 100*sum(acc_z_i > 0.315)/numel(acc_z_i), 0.315);

fft_A = fft(acc_x_i');
P2 = abs(fft_A/L);
P1 = P2(1:L/2+1);
P1(2:end-1) = 2*P1(2:end-1);
f = Fs*(0:(L/2))/L;

L = length(acc_z_i); % Length of signal
Fs = 200; % Sampling frequency
T = 1/Fs; % Sampling period
t = (0:L-1)*T; % Time vector

fft_A = fft(acc_z_i');
P2 = abs(fft_A/L);
P4 = P2(1:L/2+1);
P4(2:end-1) = 2*P4(2:end-1);
f = Fs*(0:(L/2))/L;

figure(2)
plot(f,P4)

title("Preliminary Single-Sided Amplitude Spectrum of Acceleration in Z-direction")

```

```

xlabel("f (Hz)")
ylabel("|P1(f)|")
ylim([0,0.01])

% Set parameters for pwelch function
window = hann(1024); % Window function for spectral analysis
noverlap = 4; % Number of samples to overlap between adjacent windows

% Compute the PSD of the acceleration data
[Pzz_i, f] = pwelch(acc_z_i, window, noverlap, [], Fs);

% Plot the PSD
plot(f, log(Pzz_i)); % Use log-log scale for both axes
xlabel('Frequency (Hz)');
ylabel('Power/Frequency (dB/Hz)');
title('Preliminary Power Spectral Density of Z-Acceleration Data');
grid on;

```

```

% Set parameters for pwelch function
window = hann(1024); % Window function for spectral analysis
noverlap = 4; % Number of samples to overlap between adjacent windows

[Pzz_i, f_i] = pwelch(acc_z_i, window, noverlap, [], Fs);
[Pzz_f, f_f] = pwelch(acc_z_f, window, noverlap, [], Fs);

% Plot the PSD
figure(3);
hold on
clf reset

plot(f_i, log(Pzz_i), "blue", f_f, log(Pzz_f), "red"); % Use log-log scale for both axes
%legend('Preliminary','Final')
xlabel('Frequency (Hz)');
ylabel('Log of Power/Frequency (dB/Hz)');
title('Power Spectral Density of Z-Acceleration Data');
grid on;
hold off;

```

```

L = length(acc_z_i); % Length of signal
Fs = 200; % Sampling frequency
T = 1/Fs; % Sampling period
t = (0:L-1)*T; % Time vector

fft_A_i = fft(acc_z_i');
P2 = abs(fft_A_i/L);
P4_i = P2(1:L/2+1);
P4_i(2:end-1) = 2*P4_i(2:end-1);
f_i = Fs*(0:(L/2))/L;

L = length(acc_z_f); % Length of signal
t = (0:L-1)*T; % Time vector

fft_A_f = fft(acc_z_f');
P2 = abs(fft_A_f/L);
P4_f = P2(1:L/2+1);

```



```

P4_f(2:(end-1)) = 2*P4_f(2:(end-1));

f_f = Fs*(0:(L/2))/L;

% create scatter plot with transparent markers

figure(4)

clf reset

hold on

scatter(f_i, P4_i, 50, "green", "*", 'DisplayName', 'Preliminary', 'MarkerFaceAlpha', 0.25, 'MarkerEdgeAlpha', 0.25)

scatter(f_f, P4_f, 50, "blue", "*", 'DisplayName', 'Final', 'MarkerFaceAlpha', 0.25, 'MarkerEdgeAlpha', 0.25)

title("Power Spectral Density with and Without Prototype")

xlabel("f (Hz)")

ylabel("Power")

ylim([0, 0.005])

grid on

legend('show')

hold off

```

```

DataNames = {
    'chest_cavity_preliminary_measurementscomponents.mat'...
};

legendNames = {
    'Chest'...
}; % legend name corresponds to DataName in same location

colorCell = {'g'};

% run through each data file and do something

Ax_chest = [];
Ay_chest = [];
Az_chest = [];
Amag_chest = [];
Tm_chest = [];

for i = 1:numel(DataNames)

    load(DataNames{i}) %load the data from each file

    ax = Ax(1:255800);

    ay = Ay(1:255800);

    az = Az(1:255800);

    amag = Amag(1:255800);

    tm = t(1:255800);

    Ax_chest(:,i) = ax;

    Ay_chest(:,i) = ay;

    Az_chest(:,i) = az;

    Amag_chest(:,i) = amag;

    Tm_chest(:,i) = tm;

end

Ax_chest = detrend(Ax_chest);
Ay_chest = detrend(Ay_chest);
Az_chest = detrend(Az_chest);
Amag_chest = detrend(Amag_chest);

```

```

Fs = 100; % Sampling frequency
T = 1/Fs; % Sampling period
L = length(Az_chest); % Length of signal
t = (0:L-1)*T; % Time vector

Fs = 100;
fft_A = fft(Az_chest);
P2 = abs(fft_A/L);
P1 = P2(1:L/2+1);
P1(2:end-1) = 2*P1(2:end-1);
f = Fs*(0:(L/2))/L;

load('chest_cavity_device_test_2.mat')
%%% Column 2 is Chest
Ax_all(:,1) = M2.X(1:346800);
Ay_all(:,1) = M2.Y(1:346800);
Az_all(:,1) = M2.Z(1:346800);
Amag_all(:,1) = sqrt(Ax_all(:,1).^2 + Ay_all(:,1).^2 + (Az_all(:,1).^2));
T = seconds(M2.timestamp(1:346800));
to = T(1);
t = T - to;
t = seconds(t);
Tm_all(:,1) = t / 1000;
T = 1 / Fs;
L = length(Az_all); % Length of signal
t = (0:L-1)*T; % Time vector
fft_A = fft(Az_all);
P2 = abs(fft_A/L);
P1 = P2(1:L/2+1,:);
P1(2:end-1) = 2*P1(2:end-1);
f = Fs*(0:(L/2))/L;

figure(5)
clf reset
hold on
plot(f,detrend(P1), color = 'y')
title("Single-Sided Amplitude Spectrum of Az")
xlabel("f (Hz)")
ylabel("|P1(f)|")
ylim([0,0.035])
hold off

% create scatter plot with transparent markers
figure(6)
clf reset
hold on
scatter(f, detrend(P1), 50, "magenta", "*", 'DisplayName', 'Preliminary', 'MarkerFaceAlpha', 0.25, 'MarkerEdgeAlpha', 0.25)
scatter(f_f, P4_f, 50, "red", "*", 'DisplayName', 'Final', 'MarkerFaceAlpha', 0.25, 'MarkerEdgeAlpha', 0.25)
title("PSD of of Fall 2022 And Spring 2023 Prototypes")

```

```

xlabel("f (Hz)")
ylabel("|P1(f)|")
ylim([0, 0.02])
grid on
legend('show')
hold off

```

```

% Set parameters for pwelch function
window = hann(1024); % Window function for spectral analysis
noverlap = 4; % Number of samples to overlap between adjacent windows
[Pzz_i_1, f_i_1] = pwelch(Az_all, window, noverlap, [], 100);
[Pzz_i_2, f_i_2] = pwelch(acc_z_i, window, noverlap, [], 200);
[Pzz_f, f_f] = pwelch(acc_z_f, window, noverlap, [], 200);
[Pzz_chest, f_chest] = pwelch(Ax_chest, window, noverlap, [], 100);

% Plot the PSD
figure(7);
clf reset
hold on;

plot(f_i_1, 10*log(Pzz_i_1), "magenta", f_i_2, 10*log(Pzz_i_2), "green", f_chest, 10*log(Pzz_chest), "blue", f_f, 10*log(Pzz_f), "red"); % Use
log-log scale for both axes

legend('Prelim Data 2022', 'Prelim Data 2023', 'Fall 2022 Proto.', 'Spring 2023 Proto. ');

xlabel('Frequency (Hz)');
ylabel('Log of Power/Frequency (dB/Hz)');
title('PSD of of Fall 2022 And Spring 2023 Prototypes');
grid on
hold off

```

```

L = length(Az_all); % Length of signal
Fs = 100; % Sampling frequency
T = 1/Fs; % Sampling period
t = (0:L-1)*T; % Time vector
fft_A_i = fft(Az_all');
P2 = abs(fft_A_i/L);
Pzz_i_1 = P2(1:L/2+1);
Pzz_i_1(2:end-1) = 2*Pzz_i_1(2:end-1);
f_i_1 = Fs*(0:(L/2))/L;
%[period_i_1,fperiod_i_1] = periodogram(Az_all,[],length(Az_all),100);
[plomb_i_1,f_plomb_i_1] = plomb(Az_all,t); % Compute PSD using plomb function

```

```

L = length(acc_z_i); % Length of signal
Fs = 200; % Sampling frequency
T = 1/Fs; % Sampling period
t = (0:L-1)*T; % Time vector
fft_A_f = fft(acc_z_i');
P2 = abs(fft_A_f/L);
Pzz_i_2 = P2(1:L/2+1);

```

```

Pzz_i_2(2:(end-1)) = 2*Pzz_i_2(2:(end-1));

f_i_2 = Fs*(0:(L/2))/L;

%[period_i_2,fperiod_i_2] = periodogram(acc_z_i,[],length(acc_z_i),200);

[plomb_i_2,f_plomb_i_2] = plomb(acc_z_i,t); % Compute PSD using plomb function

L = length(Ax_chest); % Length of signal

Fs = 100; % Sampling frequency

T = 1/Fs; % Sampling period

t = (0:L-1)*T; % Time vector

fft_A_f = fft(Ax_chest');

P2 = abs(fft_A_f/L);

Pzz_chest = P2(1:L/2+1);

Pzz_chest(2:(end-1)) = 2*Pzz_chest(2:(end-1));

f_chest = Fs*(0:(L/2))/L;

%[period_f_1,fperiod_f_1] = periodogram(Ax_chest,[],length(Ax_chest),100);

[plomb_chest, f_plomb_chest] = plomb(Ax_chest,t); % Compute PSD using plomb function

L = length(acc_z_f); % Length of signal

Fs = 200; % Sampling frequency

T = 1/Fs; % Sampling period

t = (0:L-1)*T; % Time vector

fft_A_i = fft(acc_z_i');

P2 = abs(fft_A_i/L);

Pzz_f = P2(1:L/2+1);

Pzz_f(2:end-1) = 2*Pzz_f(2:end-1);

f_f = Fs*(0:(L/2))/L;

%[period_f_2,fperiod_f_2] = periodogram(acc_z_f,[],length(acc_z_f),200);

[plomb_f_2, f_plomb_f_2] = plomb(acc_z_f,t); % Compute PSD using plomb function

% create scatter plot with transparent markers

figure(4)

clf reset

hold on

% scatter(f_i_2, Pzz_i_2, 50, "green", "*", 'DisplayName', 'Prelim Data 2023', 'MarkerFaceAlpha', 0.25, 'MarkerEdgeAlpha', 0.25)

% scatter(f_f, Pzz_f, 50, "blue", "*", 'DisplayName', 'Spring 2023 Proto.', 'MarkerFaceAlpha', 0.25, 'MarkerEdgeAlpha', 0.25)

scatter(f_i_1, Pzz_i_1/9.8, 50, "magenta", "*", 'DisplayName', 'Prelim Data 2022', 'MarkerFaceAlpha', 0.25, 'MarkerEdgeAlpha', 0.25)

scatter(f_chest, Pzz_chest/9.8, 50, "red", "*", 'DisplayName', 'Fall 2022 Proto.', 'MarkerFaceAlpha', 0.25, 'MarkerEdgeAlpha', 0.25)

title("PSD of Spring 2023 Data")

xlabel("f (Hz)")

ylabel("Power")

ylim([0, 0.005])

grid on

legend('show')

hold off

figure(5)

clf reset

hold on

```

```

plot(f_plomb_i_1, plomb_i_1, "magenta", f_plomb_i_2, plomb_i_2, "green", f_plomb_chest, plomb_chest, "red", f_plomb_f_2, plomb_f_2, "blue")
ylim([0 0.02])
xlabel('Cycles/Year')
ylabel('dB / (Cycles/Year)')
title('Periodogram of Relative Sunspot Number Data')
legend('Prelim Data 2022', 'Prelim Data 2023','Fall 2022 Proto.','Spring 2023 Proto.')
hold off

```

```

% create scatter plot with transparent markers

figure(9)
clf reset

hold on

scatter(f_i_2, Pzz_i_2, 50, "green", "*", 'DisplayName', 'Prelim Data 2023', 'MarkerFaceAlpha', 0.25, 'MarkerEdgeAlpha', 0.25)
scatter(f_f, Pzz_f, 50, "red", "*", 'DisplayName', 'Spring 2023 Proto.', 'MarkerFaceAlpha', 0.25, 'MarkerEdgeAlpha', 0.25)
% scatter(f_i_1, Pzz_i_1, 50, "magenta", "*", 'DisplayName', 'Prelim Data 2022', 'MarkerFaceAlpha', 0.25, 'MarkerEdgeAlpha', 0.25)
% scatter(f_chest, Pzz_chest, 50, "blue", "*", 'DisplayName', 'Fall 2022 Proto.', 'MarkerFaceAlpha', 0.25, 'MarkerEdgeAlpha', 0.25)

title("Power Spectral Density Graph Spring 2023")

xlabel("f (Hz)")
ylabel("Power")

ylim([0, .035])

grid on

legend('show')

hold off

```

```

L = length(Az_all); % Length of signal
Fs = 100; % Sampling frequency
T = 1/Fs; % Sampling period
t = (0:L-1)*T; % Time vector
N = length(Az_all); % Length of signal
xdft = fft(Az_all);
xdft = xdft(1:N/2+1);
Pzz_i_1 = (1/(Fs*N)) * abs(xdft).^2;
Pzz_i_1(2:end-1) = 2*Pzz_i_1(2:end-1);
f_i_1 = 0:Fs/length(Az_all):Fs/2;

L = length(acc_z_i); % Length of signal
Fs = 200; % Sampling frequency
T = 1/Fs; % Sampling period
t = (0:L-1)*T; % Time vector
N = length(acc_z_i); % Length of signal
xdft = fft(acc_z_i);
xdft = xdft(1:N/2+1);
Pzz_i_2 = (1/(Fs*N)) * abs(xdft).^2;
Pzz_i_2(2:end-1) = 2*Pzz_i_2(2:end-1);
f_i_2 = 0:Fs/length(acc_z_i):Fs/2;

L = length(Ax_chest); % Length of signal
Fs = 100; % Sampling frequency

```

```

T = 1/Fs; % Sampling period
t = (0:L-1)*T; % Time vector
N = length(Ax_chest); % Length of signal
xdft = fft(Ax_chest);
xdft = xdft(1:N/2+1);
Pzz_chest = (1/(Fs*N)) * abs(xdft).^2;
Pzz_chest(2:end-1) = 2*Pzz_chest(2:end-1);
f_chest = 0:Fs/length(Ax_chest):Fs/2;
L = length(acc_z_f); % Length of signal
Fs = 200; % Sampling frequency
T = 1/Fs; % Sampling period
t = (0:L-1)*T; % Time vector
N = length(acc_z_f); % Length of signal
xdft = fft(acc_z_f);
xdft = xdft(1:N/2+1);
Pzz_f = (1/(Fs*N)) * abs(xdft).^2;
Pzz_f(2:end-1) = 2*Pzz_f(2:end-1);
f_f = 0:Fs/length(acc_z_f):Fs/2;
figure(5)
clf reset
hold on
%plot(f_plomb_i_1, plomb_i_1, "magenta", f_plomb_i_2, plomb_i_2, "green", f_plomb_chest, plomb_chest, "red", f_plomb_f_2, plomb_f_2, "blue")
plot(f_i_1, Pzz_i_1, 'magenta', f_i_2, Pzz_i_2, 'green', f_chest, Pzz_chest, 'red', f_f, Pzz_f, 'blue')
ylim([0 0.001])
xlabel('Frequency (Hz)')
ylabel('Power Spectral Density')
title('Power Spectral Density using Plomb PSD and Periodogram')
legend('Plomb PSD Prelim Data 2022', 'Plomb PSD Prelim Data 2023', 'Plomb PSD Fall 2022 Proto.', 'Plomb PSD Spring 2023 Proto.', 'Periodogram Prelim Data 2022', 'Periodogram Prelim Data 2023', 'Periodogram Fall 2022 Proto.', 'Periodogram Spring 2023 Proto.')
hold off

% Set parameters for pwelch function
nfft = 1024; % Number of points for FFT
noverlap = 1; % Number of samples to overlap between adjacent windows
Fs = 100; % Sampling frequency for Az_all and Ax_chest
Fs_i = 200; % Sampling frequency for acc_z_i and acc_z_f
% Define window types to test
window_types = ["rectwin", "bartlett", "hann", "hamming"];
% Preallocate arrays to store PSD values for each window type
Pzz_i_1_all = zeros(nfft/2+1, length(window_types));
Pzz_i_2_all = zeros(nfft/2+1, length(window_types));
Pzz_f_all = zeros(nfft/2+1, length(window_types));
Pzz_chest_all = zeros(nfft/2+1, length(window_types));
for i = 1:length(window_types)
    % Generate window
    window = window_types(i);

```

```

win = eval(sprintf('%s(nfft)', window));

% Compute PSD for each signal using current window
[Pzz_i_1, f_i_1] = pwelch(Az_all, win, noverlap, [], Fs);
[Pzz_i_2, f_i_2] = pwelch(acc_z_i, win, noverlap, [], Fs_i);
[Pzz_f, f_f] = pwelch(acc_z_f, win, noverlap, [], Fs_i);
[Pzz_chest, f_chest] = pwelch(Ax_chest, win, noverlap, [], Fs);

% Store PSD values in arrays
Pzz_i_1_all(:,i) = Pzz_i_1;
Pzz_i_2_all(:,i) = Pzz_i_2;
Pzz_f_all(:,i) = Pzz_f;
Pzz_chest_all(:,i) = Pzz_chest;

end

% Plot the PSD for each window type
figure(7);
clf reset
hold on;
colors = {'magenta', 'green', 'blue', 'red'};
for i = 1:length(window_types)
    plot(f_i_1, 10*log(Pzz_i_1_all(:,i)), colors{i}, ...
         f_i_2, 10*log(Pzz_i_2_all(:,i)), colors{i}, ...
         f_chest, 10*log(Pzz_chest_all(:,i)), colors{i}, ...
         f_f, 10*log(Pzz_f_all(:,i)), colors{i}, ...
         'LineWidth', 1.2); % Use log-log scale for both axes
end

legend('Rectangular Window', 'Bartlett Window', 'Hann Window', 'Hamming Window')
xlabel('Frequency (Hz)');
ylabel('Log of Power/Frequency (dB/Hz)');
title('PSD of of Fall 2022 And Spring 2023 Prototypes');
grid on
hold off

% % Assume Pxx_i and Pxx_f are the two vectors to be compared
% % First, rank the data from both groups
% ranks_i = tiedrank(Pzz_i_1);
% ranks_f = tiedrank(Pzz_chest);
%
% % Compute the U statistic and the corresponding p-value
% [pval, h] = ranksum(ranks_i, ranks_f);
%
% % Display the results
% disp(['Mann-Whitney U Test']);
% disp(['p-value = ' num2str(pval)]);

% % Assume Pxx_i and Pxx_f are the two vectors to be compared

```

```

% % Calculate the sample means and standard deviations for both groups

% mean_i = mean(Pzz_i_2);
% mean_f = mean(Pzz_f);
% std_i = std(Pzz_i_2);
% std_f = std(Pzz_f);
%
% % Calculate the effective sample sizes for both groups
% n_i = length(Pzz_i_2);
% n_f = length(Pzz_f);
% df = (std_i^2/n_i + std_f^2/n_f)^2 / ( (std_i^2/n_i)^2 / (n_i-1) + (std_f^2/n_f)^2 / (n_f-1) );
%
% % Calculate the t-statistic and p-value
% t = abs(mean_i - mean_f) / sqrt(std_i^2/n_i + std_f^2/n_f);
% pval = 2*tcdf(-t, df);
%
% % Display the results
% disp(['Welch''s t-test results: t = ' num2str(t) ', p = ' num2str(pval)]);

```

```

% Assume Pzz_i_2 and Pzz_f are the two vectors to be compared

% Set the number of bins
numBins = 250;

% Determine the bin size for Pzz_i_2
binSize_i = ceil(length(Pzz_i_1) / numBins);
numBins_i = ceil(length(Pzz_i_1) / binSize_i);

% Determine the bin size for Pzz_f
binSize_f = ceil(length(Pzz_chest) / numBins);
numBins_f = ceil(length(Pzz_chest) / binSize_f);

% Pre-allocate arrays to store the t-test results and p-values for each bin
t_vals = zeros(numBins, 1);
p_vals = zeros(numBins, 1);

% Iterate over each bin and perform Welch's t-test
for i = 1:numBins
    % Determine the range of indices for the current bin
    idx_i = (i-1)*binSize_i+1 : min(i*binSize_i, length(Pzz_i_1));
    idx_f = (i-1)*binSize_f+1 : min(i*binSize_f, length(Pzz_chest));

    % Extract the data for the current bin
    data_i = Pzz_i_1(idx_i);
    data_f = Pzz_chest(idx_f);

    % Calculate the t-test and p-value for the current bin
    [~, p_val, ~, stats] = ttest2(data_i, data_f, 'Vartype', 'unequal');
    t_vals(i) = stats.tstat;
    p_vals(i) = p_val;
end

% Determine the number of significant bins (alpha = 0.001)

```



```
sigBins = sum(p_vals < 0.05);  
  
% Display the results  
disp(['Number of significant bins: ' num2str(sigBins)]);  
  
[~, p_val_acc, ~, stats_acc] = ttest2(acc_z_i, acc_z_f, 'Vartype', 'unequal');  
stats_acc  
  
disp(['T-test for Acceleration Data: ', num2str(p_val_acc)]);
```